

Metallabenzenes

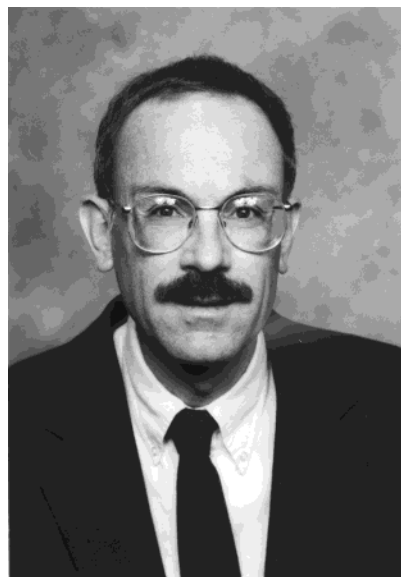
John R. Bleeke

Department of Chemistry, Washington University, St. Louis, Missouri 63130

Received July 27, 2000

Contents

I. Introduction	1205
II. Theory	1206
III. Osmabenzenes	1206
IV. Iridabenzenes	1208
V. Metal-Coordinated Iridabenzenes	1212
VI. Iridaphenols	1214
VII. Iridabenzenes Revisited	1215
VIII. Transient Metallabenzenes	1217
A. Metallabenzenes as Possible Intermediates in Reactions Leading to Cyclopentadienyl–Metal Products	1217
B. Metallabenzenes as Possible Intermediates in Other Reactions	1220
IX. Other Metal-Coordinated Metallabenzenes	1221
X. Dimetallabenzenes	1224
XI. Summary	1226
XII. Acknowledgments	1226
XIII. References	1226



John R. Bleeke was born in Port Washington, WI, in 1954. After receiving his B.A. degree from Carthage College (Kenosha, WI) in 1976, he began graduate studies at Cornell University under the direction of the late E. L. Muetterties. At Cornell and later at the University of California–Berkeley, he probed the mechanism of transition-metal-catalyzed arene hydrogenation. In 1981, he took a faculty position at Washington University in St. Louis, where he is currently Associate Professor of Chemistry and Vice Chairman of the Department of Chemistry. Dr. Bleeke's work has centered on the synthesis and reactivity of organometallic compounds, particularly those containing pentadienyl or heteropentadienyl ligands. In addition, he has a long-standing research interest in metallabenzenes and other aromatic metallacycles. He has published over 50 articles in major journals and has directed the doctoral research of 18 Ph.D. students.

I. Introduction

Ever since Kekulé's¹ intuitive idea on the structure of benzene, "aromaticity" has been one of the most vexing and yet one of the most fascinating problems in chemistry. For over a century, aromatic chemistry has challenged both the theoretician and the synthesist and has provided one of the most fruitful interplays of theory and experiment in chemistry.²

Although the term "aromaticity" remains somewhat nebulous, it is generally agreed that aromatic compounds are planar, cyclic, fully conjugated systems which possess delocalized π -electrons. This cyclically delocalized electronic structure confers special properties on aromatic compounds, including ring bond lengths which are intermediate between normal single and double bonds, diamagnetic ring currents (diatropicity) as evidenced by unusual ¹H NMR chemical shifts, and high thermodynamic stability.³

While benzene is the archetypical aromatic compound, it is now well-known that heterocyclic analogues of benzene also exhibit aromatic properties.^{2,4} These heterocyclic benzenoid compounds, in which a CH group is formally replaced by an isoelectronic heteroatom, include pyridine, phosphabenzene, ar-sabenzene, pyrylium, and thiabenzene. By comparison, relatively little is known about *metallacyclic benzenoid compounds*, i.e., benzene analogues in

which a CH group has been formally replaced by a transition metal and its associated ligands. However, during the past decade, interest in these "metallabenzenes" has significantly increased and the field has experienced a flurry of activity. Of particular interest, of course, has been the issue of whether metallabenzenes exhibit aromatic properties.

This article provides the first comprehensive review of the chemistry of transition-metal-containing metallabenzenes. It does *not* cover main-group-metal-containing heterobenzenes such as stibabenzene,⁴ bismabenzene,⁴ or gallatabenzene⁵ nor does it cover "metallaheterobenzenes", in which *both* a transition metal *and* a heteroatom reside in the six-membered ring. Examples of the latter include metallathiabenzenes,⁶ metallapyryliums,⁷ and metallapyridines.⁸

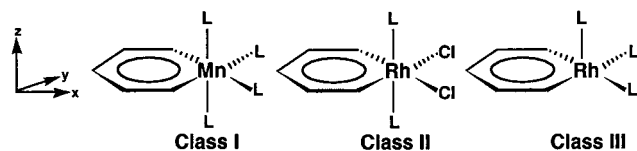
In the sections that follow, the synthesis, structure, spectroscopy, and reactivity of stable metallabenzenes, transient metallabenzenes, metallabenzenes that are π -coordinated to other metal fragments, and

dimetallabenzene are described. In each of these sections, special attention is paid to the issue of aromaticity, particularly whether the structural and spectroscopic features of these metallacycles are consistent with aromatic character. Throughout this review, metallabenzene, metal-coordinated metallabenzene, or dimetallabenzene for which there is compelling structural or spectroscopic evidence are given *compound numbers*, and these numbers are assigned sequentially. All other species, including metallabenzene that are postulated as intermediates but for which there is no hard data, are assigned *letters*.

II. Theory

Five-carbon delocalized metallacycles ("metallabenzene") were first examined theoretically by Thorn and Hoffmann in a seminal 1979 paper.⁹ Three hypothetical classes of compounds (shown in Chart 1) are identified as good candidates to exhibit the

Chart 1. Three Classes of Stable Metallabenzene Predicted by Thorn and Hoffmann^a



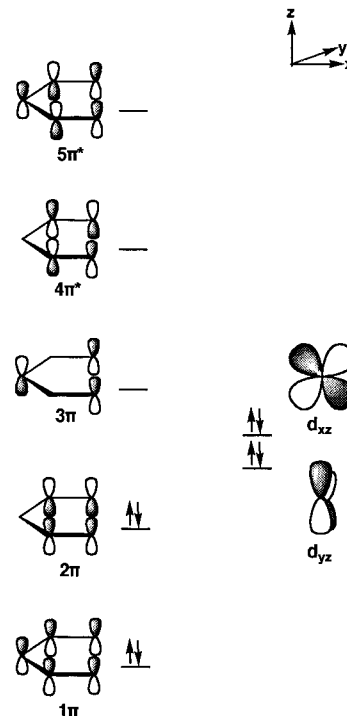
^a L is a neutral 2e⁻ donor ligand.

delocalized bonding characteristic of aromatic species. These compounds are expected to be stabilized by electron-donating ancillary ligands, L, as well as by the presence of π -donor substituents on the α and γ carbons of the ring.

In their extended Hückel calculations, Thorn and Hoffmann treat the carbon portion of the metallacycle as a monoanionic ligand (C₅H₅⁻). It serves as a 4e⁻ donor to the metal, and these electrons form the two M–C σ -bonds. In the Thorn/Hoffmann analysis, the metallacycle possesses six π -electrons and therefore obeys the Hückel $4n + 2$ rule. Four electrons reside in relatively low-lying carbon fragment π -orbitals (1 π and 2 π , Chart 2).¹⁰ The remaining two π -electrons are contributed by the filled metal d_{xz} orbital (or hybrid of appropriate symmetry), which interacts in a back-bonding fashion with the empty 3 π carbon fragment orbital (Chart 2).

Recently, Schleyer¹¹ challenged this interpretation of the π -bonding in metallabenzene. He argues that *two* filled metal d orbitals, d_{xz} and d_{yz} (or hybrids of appropriate symmetry), are strongly involved. Orbital d_{xz} interacts with empty 3 π as described above, while orbital d_{yz} interacts with filled 2 π to produce two new filled π -molecular orbitals. One of these new π -MO's is bonding between the metal and the α ring carbons while the other is antibonding. The antibonding partner is somewhat stabilized by interaction with the empty carbon fragment orbital 4 π^* (Chart 2). Hence, Schleyer concludes that metallabenzene possesses eight π -electrons which are housed in 1 π , d_{yz} + 2 π , d_{xz} - 2 π , and d_{xz} + 3 π . Interestingly, two of these π -orbitals (1 π and d_{xz} + 3 π) have Hückel character, while the remaining two have Möbius character (i.e.,

Chart 2. Five π -Orbitals for the C₅H₅⁻ Carbon Moiety and the d_{xz} and d_{yz} Metal Orbitals in a Metallabenzene^a



^a Interactions between these orbitals give rise to a cyclically delocalized π electronic structure.

the interaction between the metal d orbital and the carbon fragment is a delta or face-to-face interaction). On the basis of geometric, energetic, and magnetic criteria, Schleyer asserts that metallabenzene are aromatic but somewhat less so than benzene.¹²

III. Osmabenzene

The first example of a stable, isolable metallabenzene was reported by Roper et al. in 1982.¹³ "Osmabenzene", **1**, was synthesized by a cyclization reaction involving the thiocarbonyl (CS) ligand in precursor **A** and two ethyne molecules (Scheme 1). Closely

Scheme 1

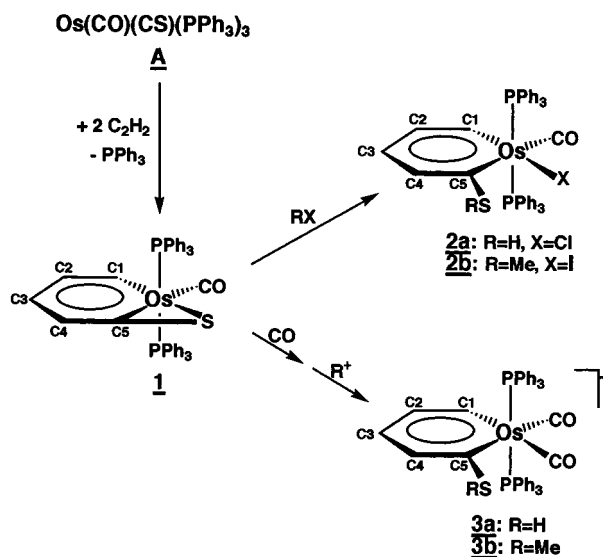


Table 1. Structural Data for Metallabenzenes^a

cmpd no.	bond distances (Å)					
	M–C1	M–C5	C1–C2	C2–C3	C3–C4	C4–C5
1	2.00(1)	2.00(1)	1.39(2)	1.42(2)	1.38(2)	1.36(2)
4a	2.011(7)	2.129(7)	1.336(10)	1.411(10)	1.347(11)	1.411(11)
4b	2.039(9)	2.128(9)	1.320(13)	1.390(14)	1.367(14)	1.418(13)
5	2.024(8)	1.985(8)	1.369(10)	1.402(11)	1.370(11)	1.392(10)
8	2.008(7)	2.008(7)	1.390(10)	1.387(10)	1.387(10)	1.390(10)
9a	1.988(24)	1.963(23)	1.378(37)	1.390(35)	1.420(39)	1.390(34)
15	2.031(16)	1.916(16)	1.352(25)	1.406(26)	1.355(26)	1.464(25)
16	2.002(12)	2.023(13)	1.371(19)	1.427(21)	1.398(22)	1.371(20)
18	2.025(8)	2.021(8)	1.33(1)	1.38(1)	1.41(1)	1.41(1)

cmpd no.	bond angles (deg)						sum
	C1–M–C5	M–C1–C2	C1–C2–C3	C2–C3–C4	C3–C4–C5	C4–C5–M	
1	88.0	126.1	125.7	127.1	118.4	134.5	719.8
4a	87.1(3)	130.0	126.6	124.7	125.9	125.3	719.6
4b	87.2(4)	129.4	126.5	127.3	123.2	126.1	719.7
5	84.7(3)	131.2(6)	122.6(7)	125.3(7)	121.8(7)	132.9(6)	718.5
8	85.7(4)	131.1(6)	123.2(8)	124.9(10)	123.2(8)	131.1(6)	719.2
9a	89.0(10)	127.9(19)	125.3(24)	124.3(23)	122.1(23)	130.7(18)	719.3
15	90.2(7)	129.1(12)	121.0(16)	129.7(16)	121.3(16)	128.4(12)	719.7
16	89.7(5)	127.6(10)	123.4(13)	128.4(14)	120.5(14)	130.0(10)	719.6
18	86.9(3)	130.7(7)	125.5(8)	124.2(8)	123.6(8)	128.8(6)	719.7

cmpd no.	metal atom displacement from metallabenzene ring, dihedral angle	
	displacement of M (Å)	dihedral angle (deg)
1	0.04	1.3
4a	0.13	5.0
4b	0.09	3.3
5	0.24	9.2
8	0.17	6.7
9a	0.13	5.3
15	<0.10	3.8
16	0.10	4.0
18	0.10	3.7

^a See schemes for atom labeling.**Table 2. NMR Chemical Shift Data for Metallabenzenes (δ)^a**

cmpd no.	H1	H2	H3	H4	H5	C1	C2	C3	C4	C5
1	13.95	7.28	7.28	7.28		X	X	X	X	X
2b	12.74	6.21	6.96	6.60		221.58	123.82	145.85	121.62	237.45
4a	14.00		7.95	7.00		222.69	144.24	138.90	124.10	X
4b	12.61		7.15	6.79		210.81	110.56	147.75	126.14	240.31
5	10.91		7.18		10.91	167.6	132.0	129.9	132.0	167.6
6a^b	10.85		7.14		10.85	167.9	132.5	129.7	132.5	167.9
6b^b	11.05		7.22		11.05	169.4	133.5	131.1	133.5	169.4
6c^b	11.26		7.37		11.26	171.6	135.2	134.7	135.2	171.6
7a	10.76		7.12		10.76	167.8	132.7	129.7	132.7	167.8
7b	11.55		7.89		11.55	169.2	135.1	133.1	135.1	169.2
8	10.62		7.10		10.62	167.9	133.1	129.1	133.1	167.9
9a	13.95		7.86		13.95	215.1	134.8	161.6	134.8	215.1
9b	13.88		7.89		13.88	215.7	134.4	162.2	134.4	215.7
10	13.02		8.16		13.02	210.8	138.3	172.3	138.3	210.8
15	10.54		7.49			179.0	132.0	165.1	126.6	219.3
16	8.95		7.50			146.3	131.2	162.1	132.7	250.8
17	9.18		7.55			164.6	134.4	165.6	131.1	246.0
18	10.79	7.79	8.44			187.49	169.46	141.16	X	187.74
19	11.00	7.91	8.25			176.04	X	X	X	189.95
20	13.31	8.01	8.57			X	X	X	X	X

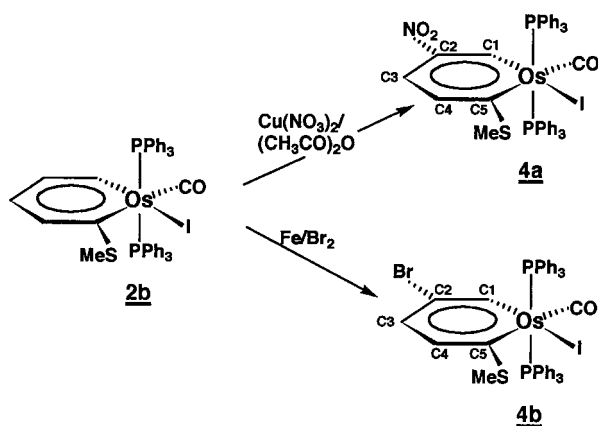
^a See schemes for atom labeling. "X" indicates that the data were not reported. ^b Rapid intramolecular ligand exchange creates apparent mirror-plane symmetry in these molecules, causing H1/H5, C1/C5, and C2/C4 to appear equivalent.

related molecules **2a,b** were generated by protonation or methylation of **1**, while osmabenzenes **3a,b** were produced by treatment of **1** with carbon monoxide, followed by protonation or methylation.

Osmabenzene **1** is a dark red-brown crystalline solid which is air stable both as a solid and in solution. X-ray structural analysis of **1** shows an essentially planar metallacycle and delocalization of bonding within the carbon portion of the ring; the

carbon–carbon bond lengths are 1.39(2), 1.42(2), 1.38(2), and 1.36(2) Å (Table 1). In addition, the Os–C bond distances are both 2.00(1) Å, intermediate in length between normal Os–C single and double bonds. In the ¹H NMR spectrum of **1**,¹⁴ the ring protons are shifted downfield; H1 resonates at δ 13.95, while the remaining three ring protons have overlapping signals near δ 7.28 (Table 2). H1's dramatic downfield shift can be attributed primarily to

Scheme 2



the magnetic anisotropic influences of the large metal atom. Such effects are often seen in transition-metal-carbenes as well as in heavy heterobenzenes such as stibabenzene or bismabenzene.⁴ However, magnetic anisotropic effects are strongly dependent on internuclear separation and decrease rapidly for protons remote from the metal center. Hence, the downfield shifts of H2–H4 are thought to result primarily from aromatic ring current effects rather than metal-based anisotropy.

Compound **1** and its relatives are best regarded as octahedral Os(II) \equiv d^6 complexes. These molecules are closely related to the octahedral d^6 complexes proposed by Thorn and Hoffmann (Classes I and II, Chart 1). As discussed in section II, the carbon portion of the ring serves as an anionic $4e^-$ σ -donor to the osmium center and also donates four electrons to the ring π -system. The remaining ring π -electrons are supplied by filled metal d orbitals. It is interesting to note that these compounds possess electron-donating ligands (PPh_3) and a π -donor substituent (S) on one of the α -carbons, both features that Thorn and Hoffmann predicted would lead to stability.

Recently, Roper et al. showed that compound **2b** undergoes electrophilic aromatic substitution reactions, specifically mononitration and monohalogenation, to produce compounds **4a,b** (Scheme 2).¹⁵ Interestingly, in both cases the SMe ring substituent exerts a strong *para*-directing effect. X-ray structures

of both substitution products have been obtained; ring planarity and delocalization of bonding are observed, as expected. However, a small disparity in the lengths of the Os–C bonds is seen, with the Os–C(SMe) bonds being about 0.1 Å longer than the Os–CH bonds in each case. This disparity may reflect the difference in trans influence exerted by the CO and I^- ligands (with CO having the stronger influence). Structural and spectroscopic data for compounds **4a,b** are summarized in Tables 1 and 2.

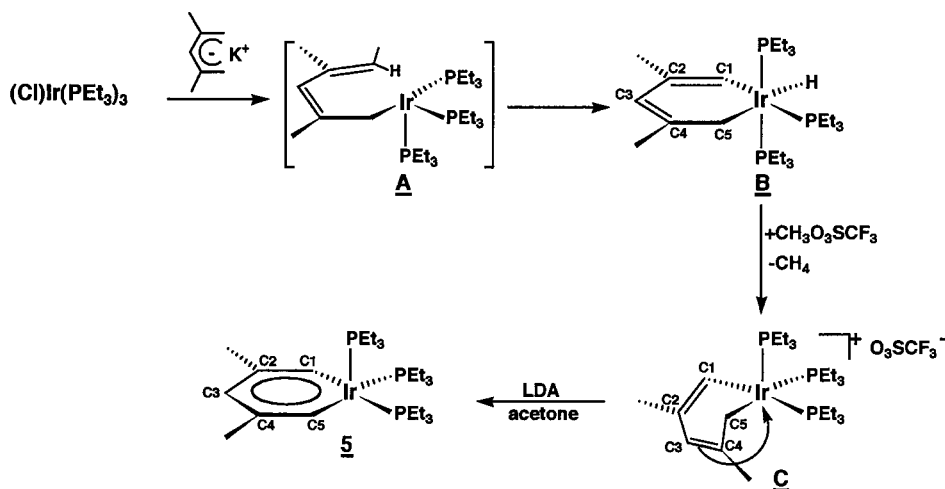
IV. Iridabenzenes

A second large family of metallabenzenes—the “iridabenzenes”—has been synthesized by Bleeke and co-workers.^{16,17} Synthesis of the parent compound, **5**, is shown in Scheme 3.¹⁸ The first step in this reaction involves formation of a transient η^1 -pentadienyl-iridium species (**A**), which undergoes C–H bond activation, producing iridacyclohexadiene–hydride, **B**. This species is then “aromatized” in two steps: (a) removal of the metal hydride with methyl triflate ($CH_3O_3SCF_3$) to produce isolable **C**, followed by (b) deprotonation of the saturated α -ring carbon (C5) with lithium diisopropylamide in acetone.

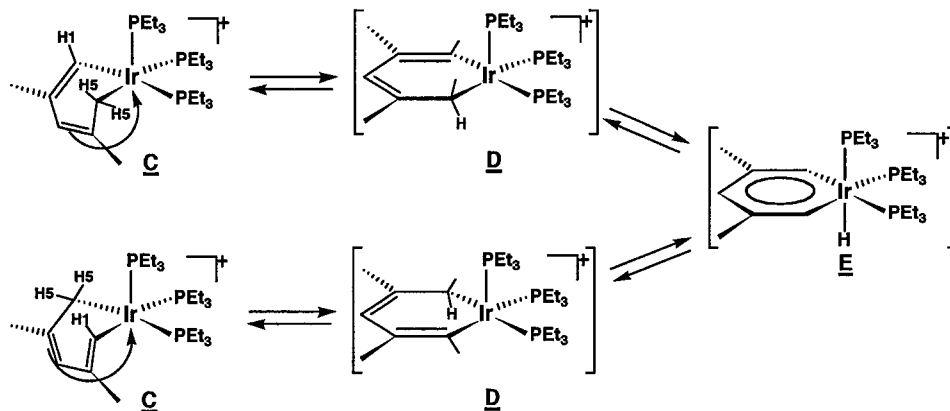
In solution, the 1,3,4,5- η -pentadienediyl-iridium species **C** exhibits a dynamic process wherein the α -hydrogens (H1 and H5's) undergo chemical exchange. As shown in Scheme 4, a likely mechanism for this fluxional process involves $16e^-$ “unhinged” iridacyclohexadiene **D** and iridabenzene–hydride **E**. The “unhinging” (dissociation of C3=C4 from the iridium center) is presumably driven by steric crowding in **C**. Given that this exchange process is occurring in solution, it follows that the *deprotonation* of **C** to form iridabenzene **5** could actually proceed from intermediates **D** or **E** or even from an agostic species on the pathway from **D** to **E**. Consistent with this idea is the observation that the less-hindered tris(PMe_3) analogue of **C** does not undergo the exchange of α -hydrogens *and* does not deprotonate to form a metallabenzene.^{16,19}

In related chemistry, Hughes^{20,21} observed the novel rearrangement shown in Scheme 5. Isotopic labeling studies have shown that this rearrangement involves an interchange of substituents between the

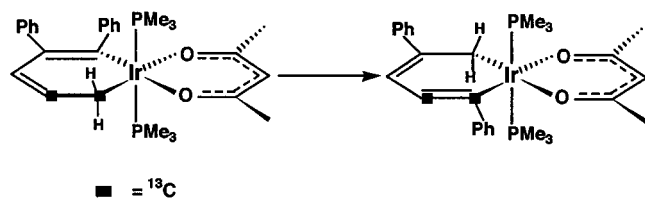
Scheme 3



Scheme 4



Scheme 5



two α -carbon atoms and is probably driven by relief of steric repulsions between adjacent phenyl groups. Hughes proposed a sequence of α -elimination/ α -addition reactions with iridabenzene intermediates. Of course, α -elimination of H or Ph from carbon to iridium requires dissociation of either a PMe_3 ligand or one arm of the acetylacetonate ligand in order to provide the required coordination site on the metal.

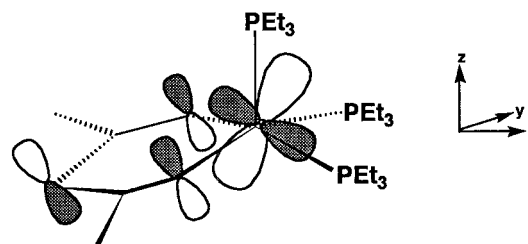
"Iridabenzene" **5** (Scheme 3) is a red crystalline solid which is stable indefinitely at room temperature under a nitrogen atmosphere. The X-ray crystal structure^{17,18} shows that the complex adopts a square pyramidal coordination geometry. The carbon portion of the metallacyclic ring is nearly planar, while the iridium atom is displaced slightly (0.24 Å) out of this plane. This displacement probably results primarily from steric interactions involving the basal phosphine ligands and the ring. The dihedral angle (or "fold angle") between planes C1/C2/C3/C4/C5 and C1/Ir/C5 is 9.2°. The internal angles around the ring sum to 718.5°, close to the value of 720° required for planar hexagon. Bonding within the ring is highly delocalized, with C–C bond distances ranging from 1.37(1) to 1.40(1) Å. The Ir–C distances of 2.024(8) and 1.985(8) Å are equivalent within experimental error and are intermediate between normal Ir–C single and double bonds. Structural data for compound **5** are summarized in Table 1.

In the ^1H NMR spectrum of **5**, the signal for H1/H5 appears as δ 10.91 while H3 resonates at δ 7.18. By comparison, H1 and H3 of the metallacyclohexadiene precursor (**B** in Scheme 3) resonate significantly upfield at δ 7.00 and 5.93, respectively. As with Roper's osmabenzene, the downfield chemical shift of H3 is thought to result primarily from the influence of an aromatic ring current while the H1/H5 shift also reflects a metal-based anisotropy. In the ^{13}C NMR spectrum of **5**, C1/C5, C2/C4, and C3 resonate at δ 167.6, 132.0, and 129.9, respectively (Table 2). The $^{31}\text{P}\{^1\text{H}\}$ NMR signal for **5** is a sharp singlet which shows no broadening even upon cooling

to -80°C . This indicates that **5** is stereochemically nonrigid and that the axial and basal phosphines are exchanging rapidly in solution, probably via a Berry-type process.

Compound **5** is the iridium analogue of the "Class III" rhodium compounds (Chart 1) that Thorn and Hoffmann predicted in their prescient 1979 paper.⁹ The $\text{C}_5\text{H}_3\text{Me}_2$ moiety is best viewed as an anionic $4e^-$ σ -donor which also contributes four electrons to the ring π -system. The remaining ring π -electrons are supplied by d orbitals on the iridium(I) center. A key π -interaction involves the filled metal hybrid d_{xz}/d_{yz} orbital and the empty 3π orbital of the carbon ligand. This interaction, pictured in Chart 3, also represents

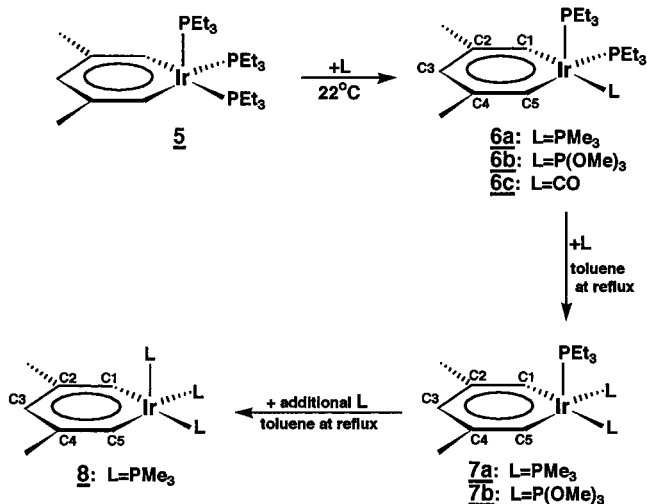
Chart 3. Key π -Interaction between the Filled Metal d_{xz}/d_{yz} Hybrid Orbital and the Empty 3π Orbital of Carbon Moiety in Compound 5



the effective HOMO for compound **5** and plays an important role in its reaction chemistry (vide infra).

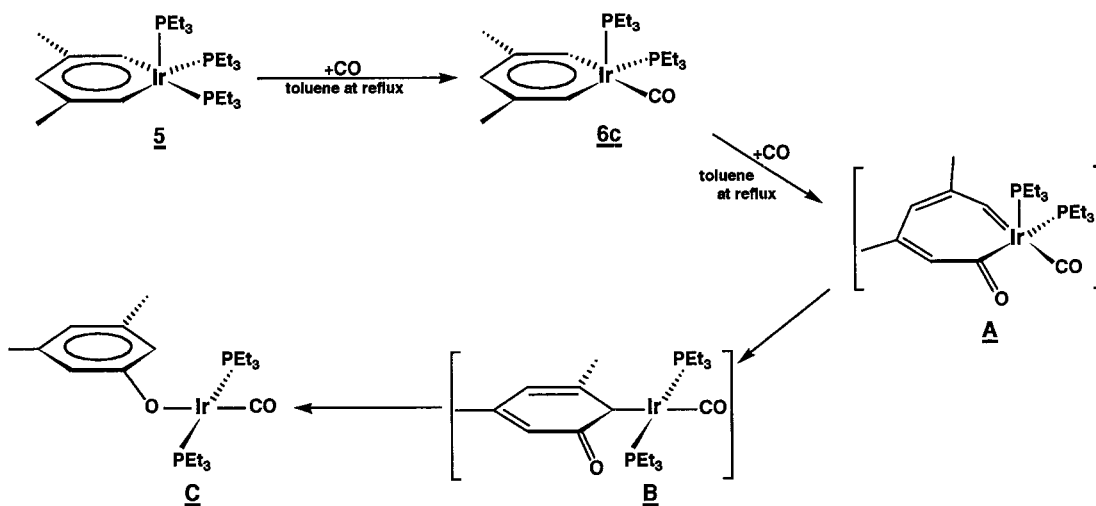
Iridabenzene **5** undergoes ligand substitution reactions with ligands, L, that are less sterically demanding than PEt_3 , including PMe_3 , $\text{P}(\text{OMe})_3$, and CO .¹⁷ At room temperature, only one PEt_3 ligand is replaced, even when excess L is employed, suggesting a dissociative mechanism (see Scheme 6). In the monosubstituted iridabenzene **6a–c**, the smaller ligand L resides in the more sterically demanding basal site. At higher temperatures (toluene at reflux), additional ligand substitution occurs with the phosphorus-based ligands, producing bis-substituted iridabenzene **7a,b** and the tris-substituted product **8** (Scheme 6). Note that only *two* $\text{P}(\text{OMe})_3$ ligands will substitute, indicating a strong electronic preference for retaining at least one good σ -donor (i.e., one PEt_3) in the iridabenzene coordination sphere. As shown in Scheme 7, treatment of **5** with excess CO in toluene at reflux leads to carbonyl insertion (**A**) and ultimately formation of a novel iridium phenoxide product, **C**.

Scheme 6

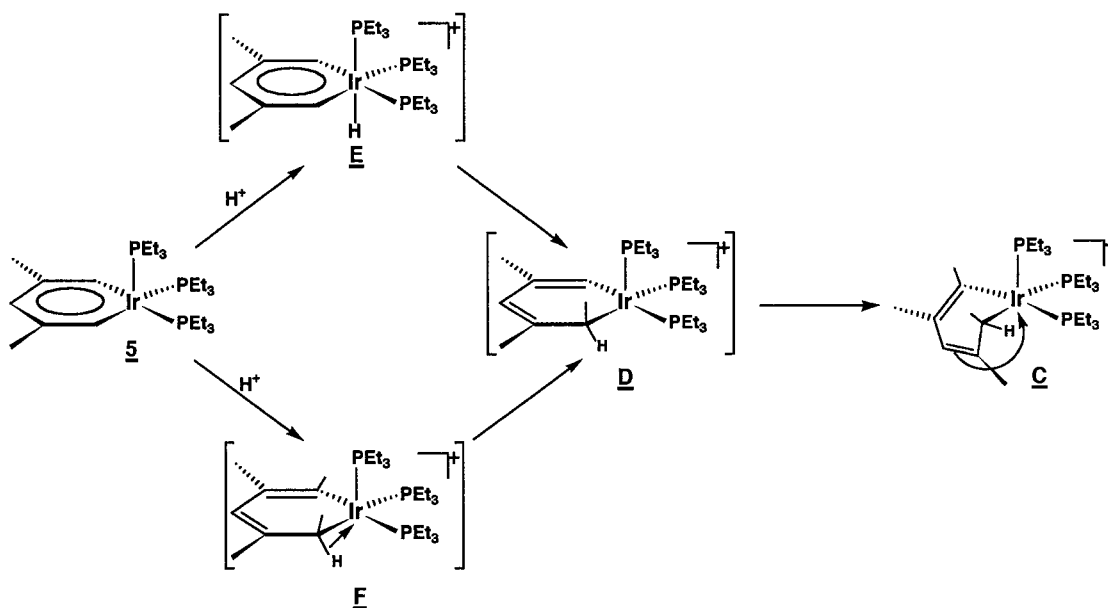


In the X-ray crystal structure of the tris(PMe₃) iridabenzene, **8**,¹⁷ the square pyramidal molecule resides on a crystallographically imposed mirror

Scheme 7



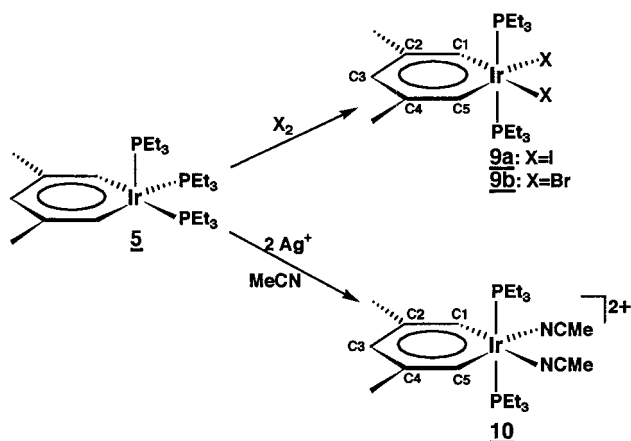
Scheme 8



plane containing the iridium atom and ring carbon C3. Bonding within the metallacyclic ring is fully delocalized; the Ir–C1, C1–C2, and C2–C3 distances are 2.008(7), 1.390(10), and 1.387(10) Å, respectively (Table 1). The ring is even more planar than in compound **5**, probably as a result of reduced steric interactions involving the basal phosphine ligands and the ring. The iridium center lies only 0.17 Å out of the plane of the five ring carbons (C1/C2/C3/C2a/C1a), while the “fold angle” between this plane and the C1/Ir/C1a plane is a mere 6.7°. The internal angles around the ring sum to 719.2°. The ¹H NMR chemical shifts for ring protons H1/H5 and H3 in **8** are δ10.62 and 7.10, respectively, similar to those in parent **5** (Table 2).

Unlike osmabenzene **2b**, compound **5** does *not* undergo classical electrophilic substitution reactions on the carbon portion of the ring. Instead, electrophiles tend to react at the accessible and very electron-rich iridium center (or Ir–C_α bond), leading ultimately to oxidation of the metal center from Ir(I) to Ir(III). For example, treatment of **5** with triflic acid (H⁺O₃SCF₃⁻) leads to regeneration of the 1,3,4,5-η-

Scheme 9



pentadienediyl complex **C** (Scheme 8), probably through the intermediacy of iridabenzene–hydride **E** or the agostic species **F**.¹⁷

Similarly, treatment of **5** with iodine (I_2) or bromine (Br_2) generates the formal oxidative addition products **9a** or **9b**, respectively (Scheme 9).^{22,23} These compounds, in which the aromatic ring is retained, are the iridium analogues of the “Class II” compounds predicted by Thorn and Hoffmann (Chart 1). They are best regarded as $\text{Ir(III)} \equiv \text{d}^6$ complexes in which the $\text{C}_5\text{H}_3\text{Me}_2$ moiety is a monoanionic $4e^-$ σ -donor. Again, the $\text{C}_5\text{H}_3\text{Me}_2$ moiety provides four electrons to the ring π -system, while metal d orbitals contribute the remaining π -electrons.

The X-ray crystal structure of **9a** confirms the octahedral coordination geometry in which the two PEt_3 ligands assume trans diaxial positions. The aromatic ring is nearly planar with the iridium atom lying just 0.13 Å out of the ring carbon plane (C1/

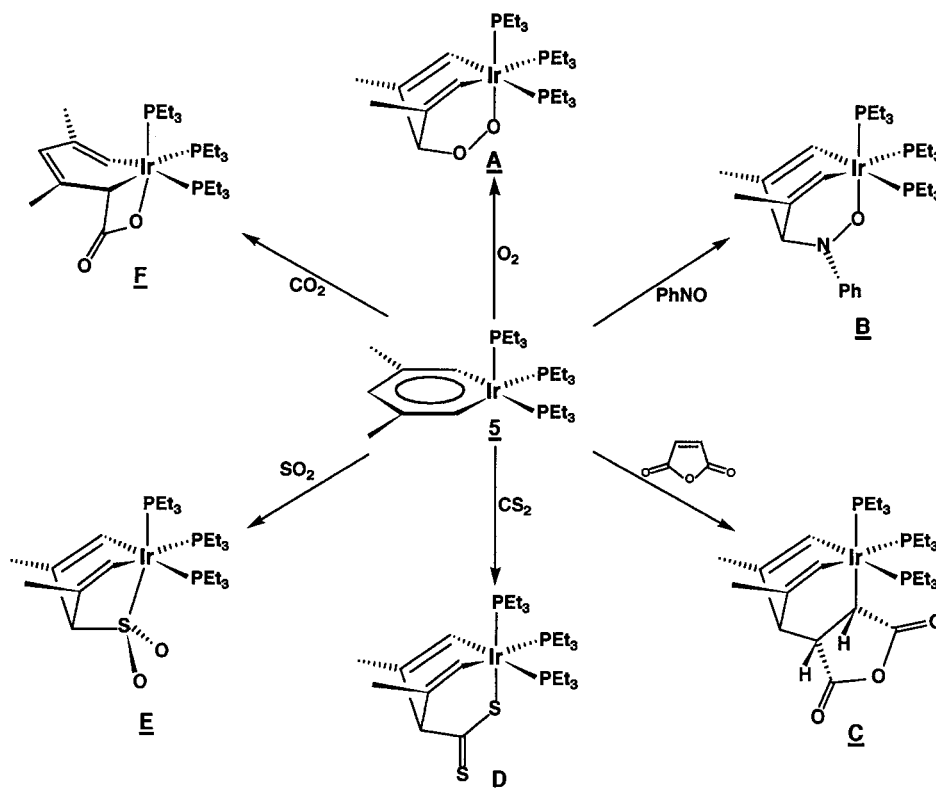
C2/C3/C4/C5). The dihedral angle between this plane and the C1/Ir/C5 plane is 5.3° . Bonding within the ring is fully delocalized (Table 1).

In the ^1H NMR, the ring protons in **9a,b** are shifted even further downfield than in compounds **5–8** (Table 2). In **9a**, for example, protons H1/H5 resonate at $\delta 13.95$ and H3 resonates at $\delta 7.86$, as compared to $\delta 10.91$ and 7.18 in compound **5**. Similar downfield shifts are observed for C1/C5 and C3 in the ^{13}C NMR spectrum. This downfield shifting probably reflects the inductive effect of an oxidized iridium center and two electronegative iodine atoms in the ring plane. The shifts are similar to those in the osmabenzene family, which are likewise d^6 octahedral complexes (vide supra).

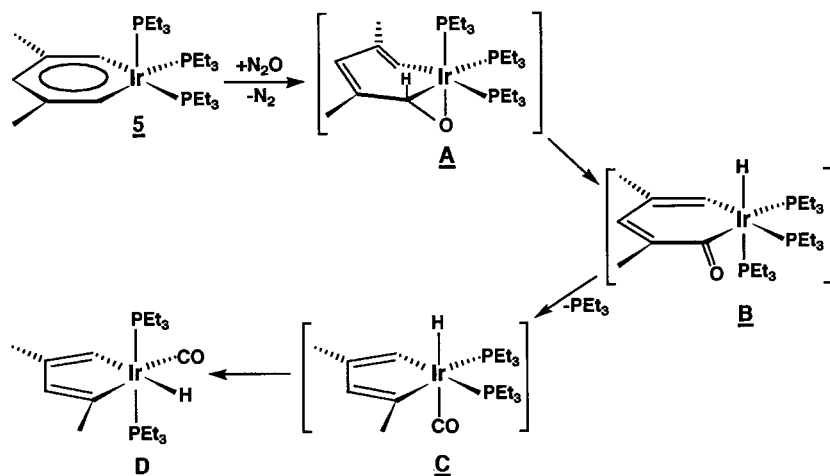
Iridabenzene **5** can also be oxidized with conventional oxidizing agents such as Ag^+ . For example, treatment of **5** with 2 equiv of Ag^+BF_4^- in acetonitrile leads to the clean production of **10** (Scheme 9). The ^1H and ^{13}C NMR spectra for **10** closely resemble those for **9a,b** (Table 2).

Iridabenzene **5** is ideally suited to participate in [4+2] cycloaddition reactions²⁴ because (a) it has a square pyramidal coordination geometry with an open face that allows close approach by substrate molecules and (b) it possesses a reactive metalladiene moiety held rigidly in a cisoid geometry. Hence, **5** reacts in a [4+2] fashion with a wide variety of cycloaddition substrates, including oxygen, nitrosobenzene, maleic anhydride, carbon disulfide, and sulfur dioxide (Scheme 10). These reactions, like those discussed above, result in a formal oxidation of the iridium center from Ir(I) to Ir(III) and are accompanied by a dramatic color change from red (iridabenzene) to light yellow (adduct). While some of these reactions may proceed via stepwise mecha-

Scheme 10



Scheme 11



nisms, the majority are thought to occur in a concerted fashion. For concerted cycloadditions, the key orbital interaction involves the effective HOMO of the electron-rich iridabenzene, pictured in Chart 3, and the LUMO of the substrate molecule, which is often a π^* orbital. Note that the wave function of the iridabenzene HOMO has opposite phases on Ir and C3, as required for a Diels–Alder-type of cycloaddition.

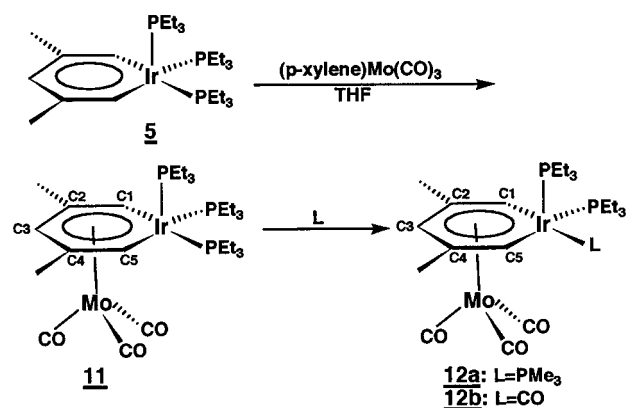
Unlike the [4+2] cycloadditions described above, iridabenzene **5** reacts with carbon dioxide (CO_2) to produce a [2+2] cycloaddition product (**F**, Scheme 10).²⁴ If this reaction is concerted, it must proceed via a perpendicular approach of the CO_2 molecule to the Ir–C $_{\alpha}$ bond, as required for a [2s + 2a] cycloaddition. The minimal steric demands of CO_2 and the presence of a second set of π -orbitals may provide stabilization for this perpendicular orientation. Alternatively, this reaction may proceed stepwise by nucleophilic attack of an iridabenzene α ring carbon on the electrophilic carbon of CO_2 , followed by iridium–oxygen bond formation. As shown in Scheme 11, nitrous oxide (N_2O) also reacts at the Ir–C $_{\alpha}$ bond, generating initially a metallaeperoxide **A**, which rearranges to a metallacyclohexadienone–hydride **B**, and ultimately retroinserts to produce the iridacyclopentadiene complex, **D**.²⁴

V. Metal-Coordinated Iridabenzenes

Iridabenzene **5** behaves more like a conventional arene in its interactions with other metal complexes. For example, treatment of $(\eta^6\text{-}p\text{-xylene})\text{Mo}(\text{CO})_3$ with **5** in tetrahydrofuran leads to clean displacement of p -xylene and production of $(\eta^6\text{-iridabenzene})\text{Mo}(\text{CO})_3$, **11** (Scheme 12).^{22,25} In compound **11**, the iridabenzene is best viewed as a $6e^-$ neutral donor (like benzene itself) and the molybdenum atom, therefore, remains an $18e^-$ center.

The X-ray structure of **11** shows that the bonding within the metallacycle is still fully delocalized, but the average Ir–C and C–C distances (2.03 and 1.41 Å, respectively) are slightly longer than those in the parent (2.00 and 1.38 Å, respectively) (see Table 3). This slight bond lengthening is expected and results from the donation of π -electron density from the ring to the Mo center. The iridium atom is displaced 0.30 Å out of the plane of the five ring carbons (C1/C2/

Scheme 12



C3/C4/C5) and away from molybdenum. The “fold angle” between this plane and the C1/Ir/C5 plane is 11.7° . The molybdenum atom is strongly π -complexed to all six atoms of the arene ring. The Mo–Ir distance is 2.978(1) Å, while the Mo–C $_{\text{ring}}$ distances range from 2.318(10) to 2.404(9) Å; the shortest bond is with C3.

The ^1H NMR signals for the ring protons in **11** shift upfield from their positions in **5**, as is normally observed when arenes coordinate to metal fragments. Protons H1/H5 appear at $\delta 8.08$ (vs $\delta 10.91$ in **5**), while H3 resonates at $\delta 6.25$ (vs $\delta 7.18$ in **5**). The ring carbons show similar upfield ^{13}C NMR shifts (see Table 4). As with conventional organic arenes, the metallabenzene moiety in **11** rotates freely with respect to the $\text{Mo}(\text{CO})_3$ fragment.²⁶ As a result, the three carbonyl groups appear to be equivalent by ^{13}C NMR, even at -80°C . The infrared spectrum of **11** shows the presence of two intense $\nu(\text{CO})$ bands (A_1 and E), as is characteristic of $(\eta^6\text{-arene})\text{Mo}(\text{CO})_3$ complexes. The very low energy of these bands (1918 and 1836 cm^{-1}) indicates substantial π -back-bonding into the carbonyl π^* orbitals and reflects the extremely electron-rich nature of arene **5**. By comparison, the $\nu(\text{CO})$ bands for $(\eta^6\text{-}p\text{-xylene})\text{Mo}(\text{CO})_3$ appear at 1975 and 1901 cm^{-1} . Since the stability of $(\eta^6\text{-arene})\text{Mo}(\text{CO})_3$ complexes increases with increasing arene basicity, it is not surprising that iridabenzene **5** cleanly displaces organic arenes from $(\eta^6\text{-arene})\text{Mo}(\text{CO})_3$ complexes in tetrahydrofuran.

Table 3. Structural Data for Metal-Coordinated Metallabenzenes^a

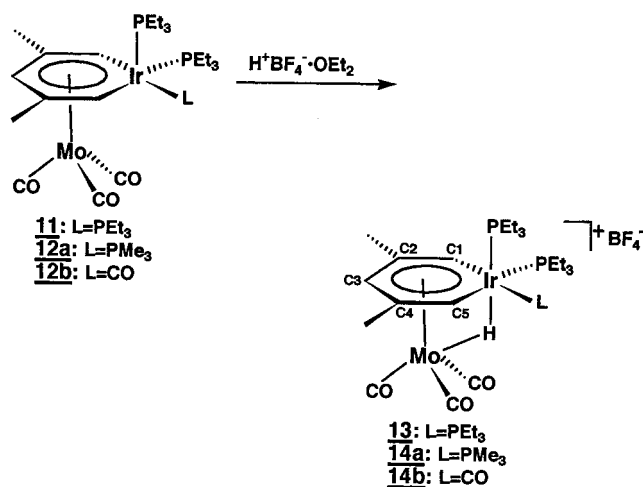
bond distances (Å)						
compd no.	M–C1	M–C5	C1–C2	C2–C3	C3–C4	C4–C5
11	2.025(8)	2.038(9)	1.399(13)	1.411(14)	1.429(13)	1.393(12)
12a	2.031(6)	2.027(6)	1.409(9)	1.395(10)	1.422(9)	1.409(9)
14a	2.058(5)	2.053(5)	1.383(7)	1.429(8)	1.410(8)	1.384(7)
24	2.072(5)	2.051(5)	1.426(6)	1.430(6)	1.423(7)	1.418(7)
25a	2.150(5)	2.161(4)	1.418(7)	1.424(6)	1.410(7)	1.404(6)
26	1.983(3)	1.983(3)	1.420(5)	1.425(5)	1.425(5)	1.420(5)
27	1.867(9)	1.838(9)	1.38(1)	1.42(1)	1.46(1)	1.41(1)
28						
ring 1	2.076(3)	2.062(3)	1.401	1.417	1.431	1.410
ring 2	2.070	2.075	1.394	1.432	1.400	1.405
29	1.970(3)	1.970(3)	1.406(4)	1.417(3)	1.417(3)	1.406(4)
bond angles (deg)						
compd no.	M'–M	M'–C1	M'–C2	M'–C3	M'–C4	M'–C5
11	2.978(1)	2.397(8)	2.404(9)	2.318(10)	2.355(9)	2.349(9)
12a	2.950(1)	2.390(6)	2.363(7)	2.336(6)	2.384(6)	2.380(6)
14a	2.854(2)	2.329(5)	2.367(5)	2.279(6)	2.351(6)	2.334(5)
24	2.729(1)	2.147(4)	2.286(4)	2.335(5)	2.315(5)	2.134(5)
25a	2.989(1)	2.297(5)	2.377(5)	2.329(4)	2.369(4)	2.310(4)
26	2.767(1)	2.146(3)	2.193(4)	2.173(5)	2.193(4)	2.146(3)
27	2.554(1)	2.111	2.223	2.242	2.234	2.103
28						
ring 1	2.831(2)	2.175	2.246	2.202	2.258	2.180
ring 2	2.812(2)	2.180	2.262	2.202	2.244	2.179
29	2.8983(3)	2.290(3)	2.175(3)	2.134(4)	2.175(3)	2.290(3)
bond angles (deg)						
compd no.	C1–M–C5	M–C1–C2	C1–C2–C3	C2–C3–C4	C3–C4–C5	C4–C5–M
11	85.1(4)	132.2(7)	121.2(8)	125.8(8)	121.8(8)	131.0(7)
12a	85.7(3)	131.0(5)	122.9(6)	125.7(6)	121.6(6)	131.5(5)
14a	85.6(2)	131.4(4)	120.9(5)	127.6(5)	121.5(5)	131.5(4)
24	91.9(2)	119.8(3)	121.1(4)	131.1(4)	122.3(4)	118.5(3)
25a	79.9(2)	133.8(3)	120.7(4)	127.4(4)	121.1(4)	134.2(3)
26	91.5(2)	123.7(3)	120.8(4)	129.2(5)	120.8(4)	123.7(3)
27	92.4(6)	128.4	122.1	123.3	120.4	128.6
28						
ring 1	83.7	131.3	121.6	125.9	121.3	131.2
ring 2	83.3	132.4	121.0	125.7	122.5	131.1
29	89.0(1)	129.0(2)	123.2(3)	124.1(3)	123.2(3)	129.0(2)
metal atom displacement from metallabenzene ring, dihedral angle						
compd no.	displacement of M (Å)			dihedral angle (deg)		
11	0.30			11.7		
12a	0.24			9.5		
14a	0.20			7.7		
24	0.80			33.6		
25a	0.33			11.6		
26	0.63			27.0		
27	0.36			16.4		
28						
ring 1	0.39			15.1		
ring 2	0.34			12.9		
29	0.32			13.0		

^a See schemes for atom labeling.**Table 4. NMR Chemical Shift Data for Metal-Coordinated Metallabenzenes (δ)^a**

compd no.	H1	H2	H3	H4	H5	C1	C2	C3	C4	C5
11	8.08		6.25		8.08	135.7	107.9	99.5	107.9	135.7
12a	8.35		6.32		7.83	140.1	108.4	99.9	106.9	132.5
12b	8.52		6.28		7.75	143.9	110.4	99.3	107.4	125.1
13	7.89		7.01		7.89	132.9	114.5	98.4	114.5	132.9
14a	7.92		7.06		7.98	134.0	114.7	98.8	114.7	132.5
14b	7.49		6.97		8.19	125.5	117.1	99.0	114.0	124.1
24			4.69			130.7	109.0	90.2	108.6	118.9
25a	8.31		5.74		6.91	165.9	X	X	X	154.5
25b	9.16		5.98		6.87	182.2	X	X	X	156.3
25c	8.67		5.95		6.85	185.7	X	X	X	158.1
26	10.31		5.47		10.31	178.5	102.2	95.6	102.2	178.5
27	9.7		5.7		9.7	167.7	103.8	91.9	103.8	167.7
28	5.62		6.23		5.62	128.3	111.3	94.4	111.3	128.3
29	9.75	4.94	4.32	4.94	9.75	177.0	86.8	83.4	86.8	177.0

^a See schemes for atom labeling. "X" indicates that the data were not reported.

Scheme 13



Like iridabenzene **5** itself, compound **11** undergoes ligand substitution reactions when treated with ligands that are less sterically demanding than PEt₃, although higher temperatures are required.²⁵ For example, treatment of **11** with PMe₃ or CO in refluxing tetrahydrofuran or acetone results in clean replacement of one PEt₃ ligand, producing **12a,b** (see Scheme 12). These species can also be produced via arene exchange by treating preformed ligand-substituted iridabenzene (**6a,c**) with (η^6 -*p*-xylene)Mo(CO)₃ in tetrahydrofuran. The unique ligand, L, in compounds **12a,b** resides in the more sterically crowded basal site. X-ray structural data and NMR data for **12a,b** are summarized in Tables 3 and 4, respectively. In solution, the iridabenzene rings in **12a,b** undergo facile rotation with respect to the Mo(CO)₃ fragment, causing the CO ligands on molybdenum to appear to be equivalent by ¹³C NMR.²⁶

When complexes **11** and **12a,b** are treated with H⁺BF₄⁻·OEt₂, protonation occurs at the metal centers, leading to production of the novel heterobimetallic μ -hydride complexes, **13** and **14a,b** (see Scheme 13).²⁵ The structure of compound **14a** has been confirmed through a low-temperature (−150 °C) X-ray diffraction study. Ring bond distances and angles are reported in Table 3. The ring in **14a**

remains delocalized, but the Ir–C_α bond distances are slightly longer than those in unprotonated **12a** (Ir–C_{ave} = 2.056 vs 2.029 Å), perhaps reflecting a weakening of the Ir–C_α π -interaction upon protonation.

The NMR spectra of **13** and **14a,b** bear a close resemblance to those of their unprotonated parents and are summarized in Table 4. Interestingly, rotation of the iridabenzene ligand in **13** and **14a,b** is still observed by ¹³C NMR at room temperature but can be arrested by cooling to −30 °C. The free energy of activation (ΔG^\ddagger) for arene rotation in **13** is calculated from variable temperature ¹³C NMR (CO) line shapes to be 13.7(4) kcal/mol.²⁶

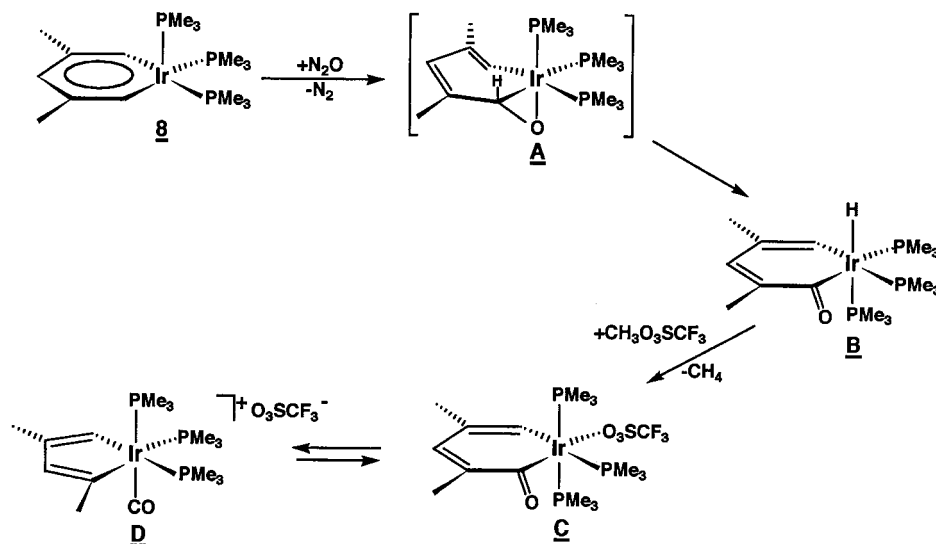
VI. Iridaphenols

As discussed earlier, treatment of iridabenzene **5** with N₂O leads to formation of an iridaepoxide, which rearranges to an iridacyclohexadienone–hydride (cf. Scheme 11). This species then rapidly loses a phosphine and reinserts to form an iridacyclopentadiene–carbonyl–hydride product. In the analogous reaction involving tris(PMe₃) iridabenzene, **8**, the iridacyclohexadienone–hydride intermediate (**B**, Scheme 14) can be isolated, presumably because phosphine dissociation is much slower in this case.²⁷ Treatment of **B** with methyl triflate (CH₃O₃SCF₃) removes the hydride ligand, generating iridacyclohexadienone **C**. When **C** is dissolved in acetone, it establishes an equilibrium with the iridacyclopentadiene–carbonyl compound **D**, a process which involves dissociation of the labile triflate ligand and reversible reinsertion of the carbonyl group.

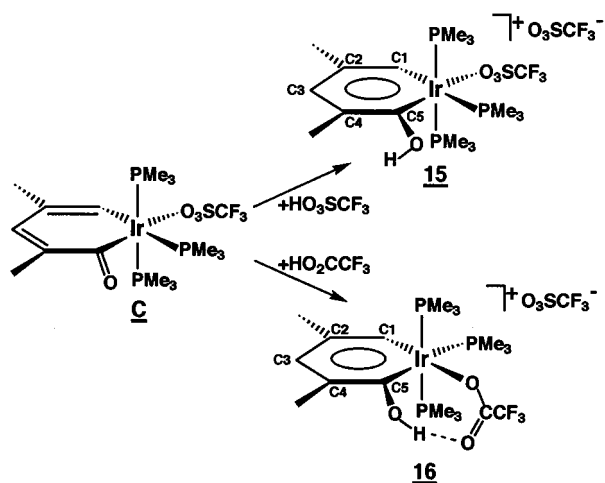
Treatment of iridacyclohexadienone **C** with acids leads to protonation at the carbonyl oxygen and the production of stable iridaphenols.²⁷ For example, when **C** is reacted with triflic acid (H⁺O₃SCF₃⁻) in tetrahydrofuran, the solution immediately turns from yellow to dark red-orange, signaling the formation of iridaphenol **15** (see Scheme 15).

The aromatization of the ring in **15** is indicated by the downfield shifting of ring protons H1 and H3. H1 moves downfield from δ 9.25 in precursor **C** to δ 10.54 in **15**, while H3 shifts from δ 6.66 to 7.49. Significant

Scheme 14



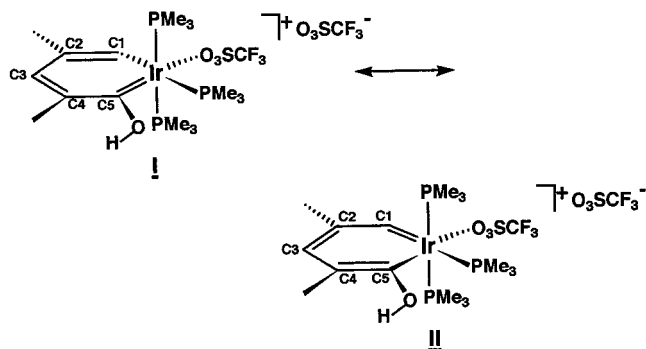
Scheme 15



downfield shifts are also observed in the ^{13}C NMR for ring carbons C1, C3, and C5 (see Table 2).

The X-ray crystal structure of **15** shows that the ring carbon-carbon bonds have moved toward equalization. Bonds C1-C2, C2-C3, C3-C4, and C4-C5 exhibit distances of 1.352(25), 1.406(26), 1.355(26), and 1.464(25) Å, respectively. The phenol carbon-oxygen bond (C5-O) has lengthened from 1.197(25) Å in precursor **C** to 1.331(20) Å in **15**. Furthermore, the iridium-carbon bonds, Ir-C1 and Ir-C5, have shortened to 2.031(16) and 1.916(16) Å, respectively, from their values of 2.052(17) and 1.987(19) Å in **C**, indicating significant metal participation in ring π -bonding. While the trend toward delocalization is clear, the small differences observed in bond distances within the ring appear to be real. This suggests that of the two resonances shown in Chart 4, structure **I** contributes more strongly than **II** to

Chart 4. Resonance Structures for Compound 15



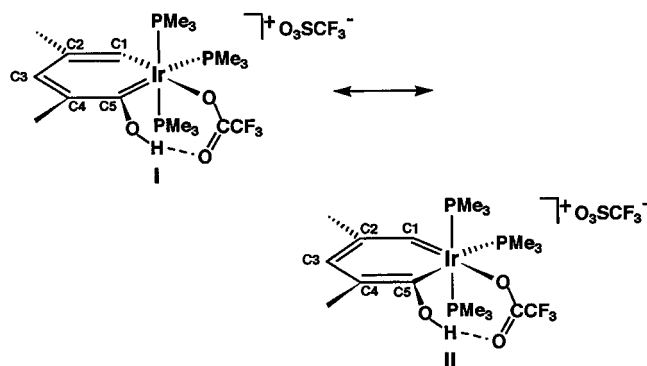
the bonding in **15**, perhaps due to heteroatom (oxygen) stabilization of the metal carbene in **I**. In addition, the weak trans influence of the triflate ligand (trans to C5) reinforces the short Ir-C5 distance. The iridaphenol ring in **15** is nearly planar; the iridium atom resides less than 0.1 Å out of the best plane made by ring carbons C1/C2/C3/C4/C5, and the dihedral angle between this plane and the C1/Ir/C5 plane is a mere 3.8°. The sum of the internal angles within the ring is 719.7°, close to the value of 720° required for a planar hexagon.

Treatment of iridacyclohexadienone **C** with trifluoroacetic acid ($\text{H}^+\text{O}_2\text{CCF}_3^-$) also leads to the

production of an iridaphenol, **16** (see Scheme 15).²⁷ This reaction is accompanied by exchange of the triflate ligand for a trifluoroacetate ligand, which coordinates cis to C5 (trans to C1), allowing intramolecular hydrogen bonding to occur between the phenol hydrogen and the carbonyl oxygen of the trifluoroacetate group.

Bonding within the metallacycle in **16** is even more highly delocalized than in **15**. The Ir-C1 and Ir-C5 distances are nearly identical at 2.002(12) and 2.023(13) Å, respectively, while ring C-C bonds C1-C2, C2-C3, C3-C4, and C4-C5 exhibit distances of 1.371(19), 1.427(21), 1.398(22), and 1.371(20) Å, respectively. Hence, it appears that resonance structures **I** and **II** (Chart 5) contribute almost equally to

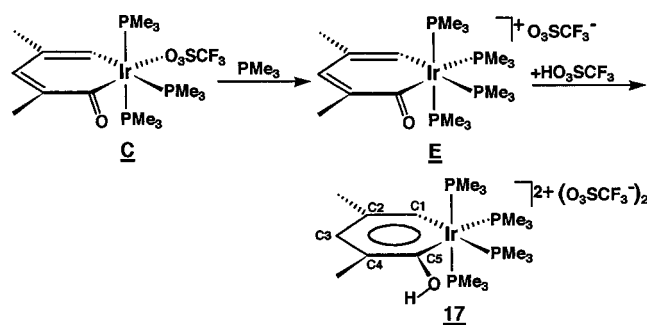
Chart 5. Resonance Structures for Compound 16



the bonding in compound **16**. Structure **I** may be stabilized by the presence of a heteroatom (oxygen) on the carbene carbon, while structure **II** probably benefits from the weaker trans influence of the trifluoroacetate group.

As shown in Scheme 16, treatment of iridacyclohexadienone **C** with PMe_3 , followed by protonation with triflic acid, generates iridaphenol **17**.²⁷ Again, comparison of the ^1H NMR spectrum of **17** with that of precursor **E** shows significant downfield shifting of ring protons H1 and H3, consistent with aromatization of the ring. In the ^{13}C NMR, downfield shifts of 20–30 ppm are observed for ring carbons C1, C3, and C5 (Table 2).

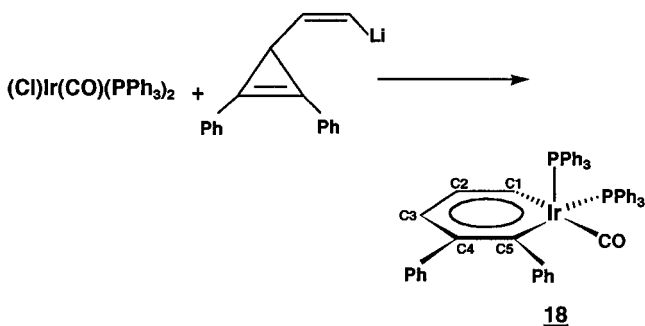
Scheme 16



VII. Iridabenzenes Revisited

Recently, Haley et al.²⁸ developed a new synthetic approach to iridabenzenes, utilizing a lithiated 3-vinyl-1-cyclopropene reagent as the source of ring carbon atoms (Scheme 17). The advantages of this approach are that it yields the iridabenzene directly

Scheme 17



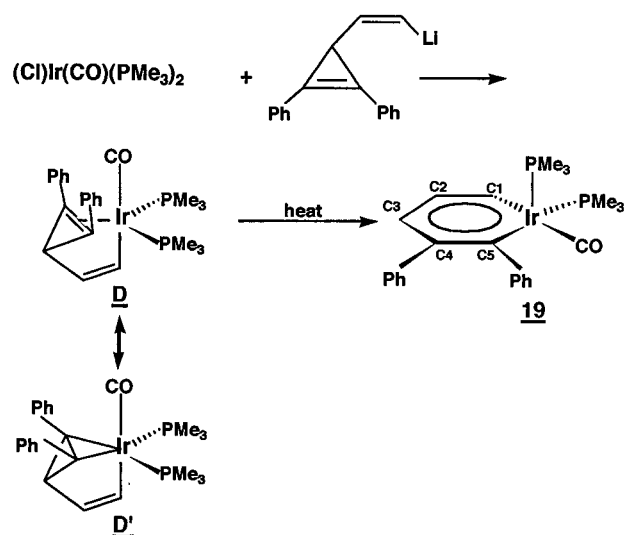
and that it could potentially be extended to prepare metallabenzene with different transition metals. A likely reaction pathway involves initial substitution of the chloride ligand in $(\text{Cl})\text{Ir}(\text{PPh}_3)_2(\text{CO})$ by the vinyl lithiate to give **A**, Scheme 18. The free cyclopropene in **A** could coordinate to the iridium center through the cyclopropene π -bond to give intermediate **B**, which could then rearrange directly to iridabenzene **18**. Alternatively, **A** or **B** could first rearrange to valence isomer **C** (Dewar iridabenzene) by insertion of iridium into one of the cyclopropene σ -bonds before converting to **18**.

The solid-state structure of **18** is similar to the iridabenzene reported earlier by Bleeke (*vide supra*). The coordination geometry is a distorted square pyramid with the small CO ligand occupying one of the basal sites. The ring is essentially planar, and the π -bonding is delocalized (see Table 1). The ^1H NMR spectrum shows the expected downfield shifting for ring protons H1, H2, and H3 (see Table 2). Compound **18** is air stable but does react with maleic anhydride to produce a [4+2] cycloaddition product.

When $(\text{Cl})\text{Ir}(\text{PMe}_3)_2(\text{CO})$ is treated with the lithiated 3-vinyl-1-cyclopropene reagent, species **D** (Scheme 19) can be isolated as a stable product at room temperature.²⁹ The X-ray structure of **D** shows an elongated π -bond, indicating substantial metal \rightarrow olefin π -back-bonding and a significant contribution from the metallabicyclobutane resonance structure, **D'**. Hence, from a structural point of view, **D** can be regarded as the first example of an "iridabenzvalene".

When **D** is heated in benzene at reflux, it converts cleanly and quantitatively to iridabenzene **19** (Scheme 19). As before, several pathways for this conversion

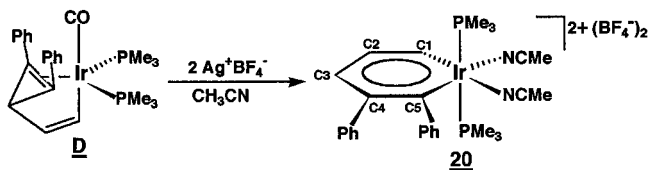
Scheme 19



can be envisaged. The simplest is concerted rearrangement of the metallabicyclobutane moiety, which would give iridabenzene directly. Alternatively, the conversion may proceed through the intermediacy of a Dewar iridabenzene valence isomer.

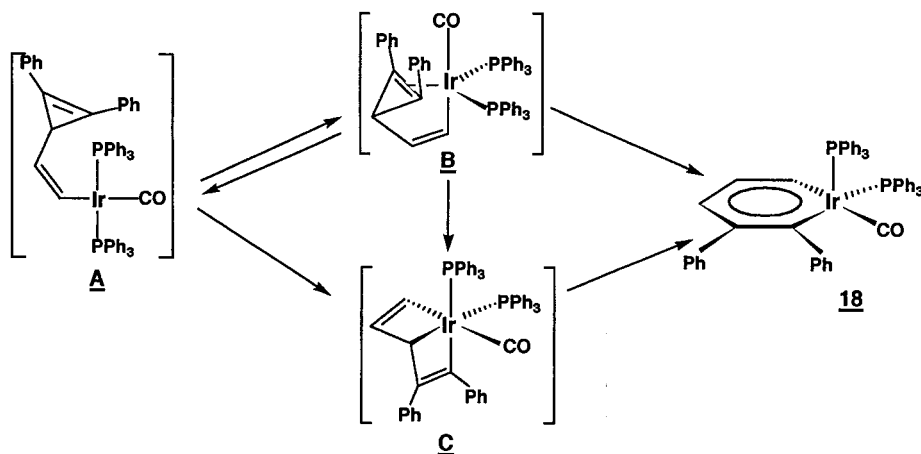
Treatment of **D** with 2 equiv of Ag^+BF_4^- in acetonitrile yields octahedral iridabenzene **20** (Scheme 20).²⁹ This species is a close analogue of compound

Scheme 20



10, reported earlier by Bleeke (*cf.* Scheme 9). Since this reaction occurs at room temperature (while the conversion of **D** to **19** requires heating), the silver reagent must be promoting the isomerization of **D**. Haley suggests a mechanism in which Ag^+ breaks one of the cyclopropene σ -bonds in **D**. The resulting intermediate rearranges to iridabenzene **19**, which is then oxidized by 2 equiv of Ag^+ to dicationic iridabenzene **20**. NMR data for this compound are reported in Table 2.

Scheme 18



VIII. Transient Metallabenzenes

A. Metallabenzenes as Possible Intermediates in Reactions Leading to Cyclopentadienyl–Metal Products

Short-lived metallabenzenes have been postulated (and sometimes observed spectroscopically) in a variety of reactions that ultimately lead to cyclopentadienyl–metal products. For example, Jones and Allison³⁰ generated the transient ruthenaphenoxide complex **21** (Scheme 21) from interligand attack of the lithiated butadienyl group in **A** on a carbonyl ligand. Although compound **21** can also be regarded as a ruthenium–acyl compound (resonance structure **21'**), the downfield ¹³C NMR chemical shift of carbon C5 (δ 293) suggests that the enolate resonance structure dominates. Compound **21** is stable to about 0 °C.

Alkylation of the ruthenaphenoxide oxygen in **21** with triethyloxonium tetrafluoroborate ($\text{Et}_3\text{O}^+\text{BF}_4^-$) produces a transient ruthenabenzene, **22** (Scheme 21), which is reasonably stable at -50 °C but rearranges by “carbene migratory insertion” at -30 °C to the η^3 -cyclopentadienyl complex **B**.³⁰ Addition of CO generates the stable σ -cyclopentadienyl product, **C**. Unfortunately, the thermal instability of **22** has prevented full NMR characterization. However, the ring protons (H2 and H3) appear to resonate between δ 7.40 and 7.80, consistent with an aromatic ring current. It is interesting to note that **22** is significantly more stable than its ruthenaphenanthrene analogue. When the ruthenaphenanthrene oxide, **23** (Scheme 22), was ethylated with $\text{Et}_3\text{O}^+\text{BF}_4^-$ at about -50 °C, no evidence for the ruthenaphenanthrene (**E**)

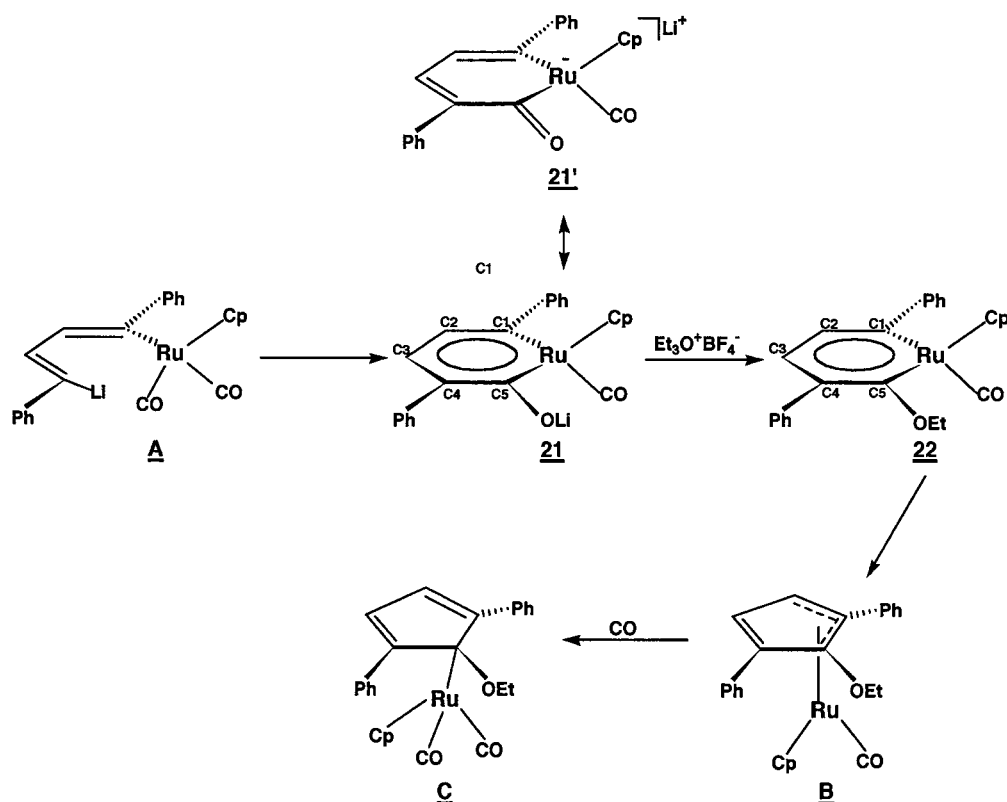
could be found; only the rearranged π -benzyl complex **F** was observed. Jones and Allison speculate that the enhanced stability of ruthenabenzene **22** versus its ruthenaphenanthrene analogue may be due to its greater aromaticity, just as benzene is more stabilized by aromaticity than is the central ring in phenanthrene.

The Allison group^{31–33} proposed four other metallaphenoxides or metallaphenanthrene oxides (**J**, **K**, **P**, **Q** in Schemes 23 and 24) as intermediates in reactions involving metal carbonyls and lithiated butadiene or biphenyl reagents. However, none of these postulated metalla-aromatic intermediates has ever been observed directly.

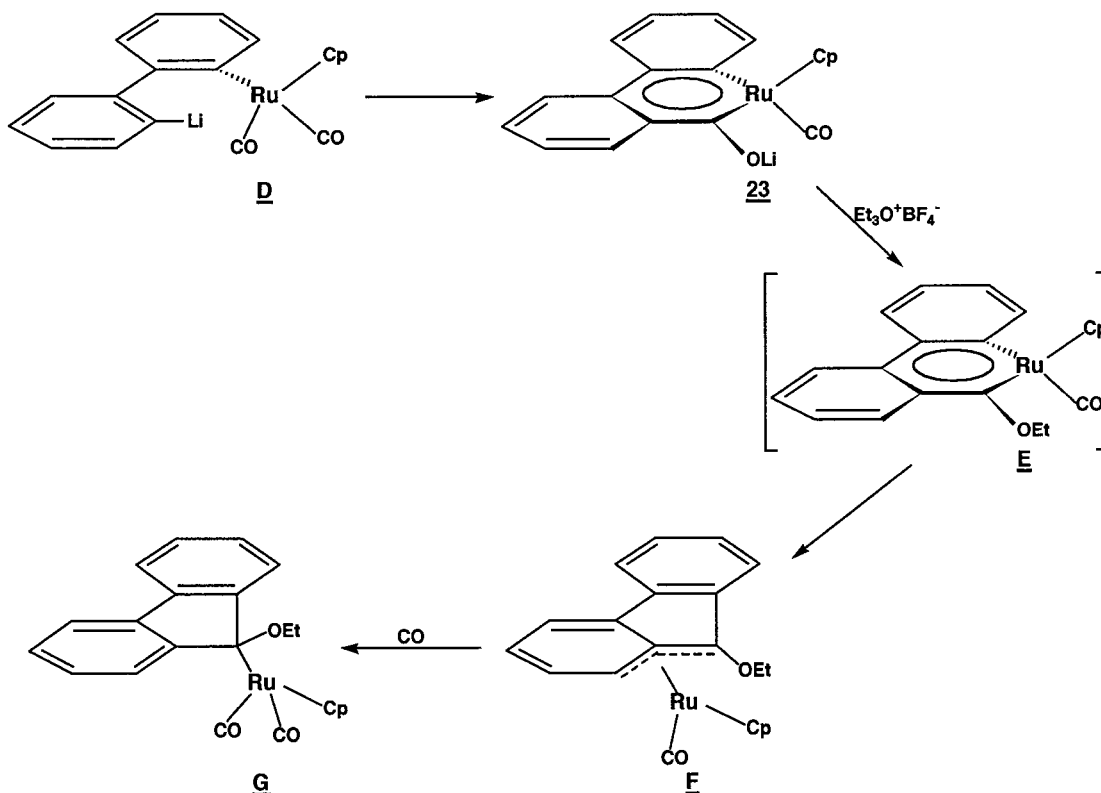
The proposed reaction sequence generating metallaphenoxides **J** and **K** (Scheme 23) involves attack of a lithiated butadienyl ligand on a carbonyl ligand.^{31,32} As in the ruthenium chemistry described above, carbene migratory insertion leads ultimately to the formation of isolable cyclopentadienyl–metal products. Methylation of the oxygen center could occur before or after the carbene migratory insertion step. Putative rhenaphenanthrene oxides **P** and **Q**³³ (Scheme 24) are formed similarly from lithiated biphenyl and carbonyl ligands but decompose directly to 9-fluorenone by reductive elimination.

In related chemistry, Jones³⁴ postulated metallaphenol intermediates in the thermal conversion of metallaindenes to indenyl–metal complexes. As shown in Scheme 25, a likely pathway for this conversion involves CO insertion into the metallaindene ring in **A** to generate **B**, followed by enolization to produce metallaphenol **C**. Carbene migratory insertion would then lead to **D** and ultimately to the observed

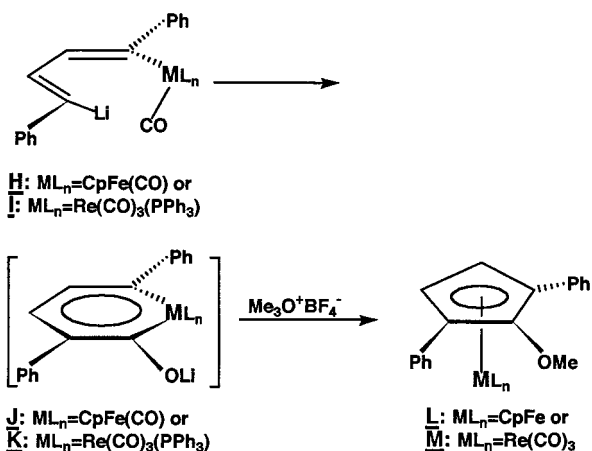
Scheme 21



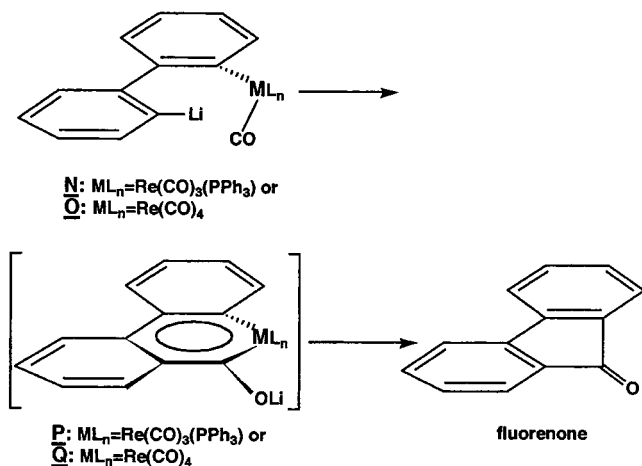
Scheme 22



Scheme 23



Scheme 24



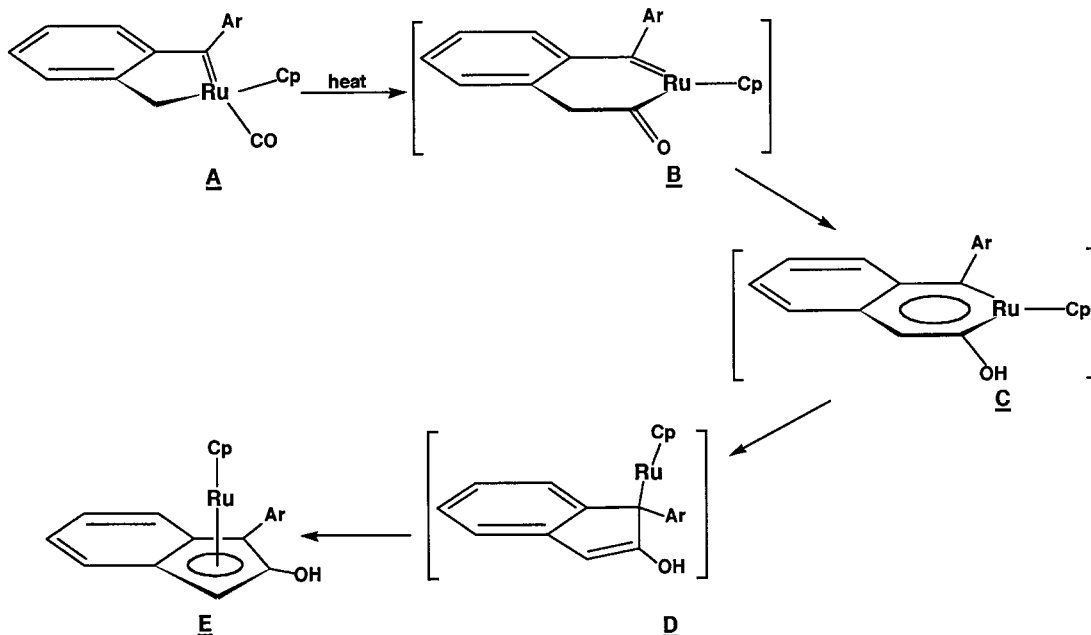
indenyl–metal product, **E**. An alternative mechanism, which involves carbene insertion into the metal–acyl bond in **B** and bypasses metallaphenol **C**, cannot be ruled out.

Schrock³⁵ suggested that metallabenzenes might be involved as intermediates in the reactions of metallacyclobutadienes with alkynes. For example, treatment of metallabutadiene **A** (Scheme 26) with 2-butyne leads to the formation of the cyclopentadienyl–metal complex **E**, perhaps through the intermediacy of metallabenzene **C**. In this case, alkyne insertion into a metallacyclobutadiene M–C bond is proposed, followed by carbene migratory insertion. An alternative mechanism involves the formation of a Dewar metallabenzene intermediate (**D**, Scheme 26), followed by reductive elimination.

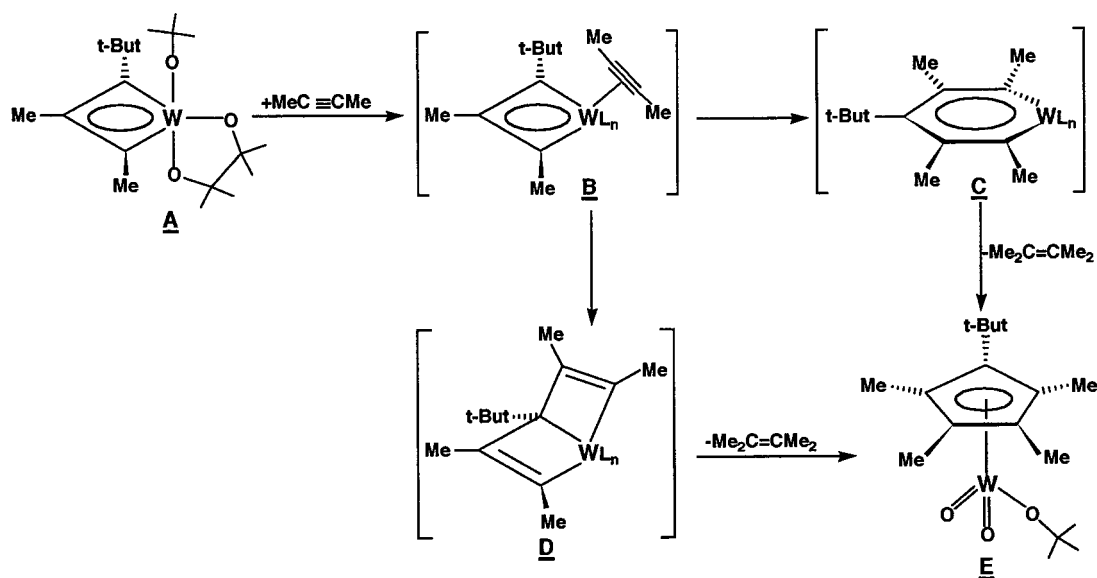
Interestingly, when metallacyclobutadiene **A** is treated with 3-hexyne, two isomeric products are formed (**F** and **G**, Scheme 27).³⁵ These species differ in the pattern of the substituents around their cyclopentadienyl rings. This skeletal scrambling implies that the initially formed metallabenzene or Dewar metallabenzene intermediates can isomerize (probably via metallacyclobutadiene–alkyne complexes) before cyclopentadienyl ring closure (vide infra).³⁶

Hughes³⁷ proposed the intermediacy of Dewar metallabenzenes in the skeletal rearrangement of an η^5 -oxacyclohexadienyl ligand to an η^5 -cyclopentadienyl ligand. As shown in Scheme 28, flash vacuum thermolysis of **A** leads to extrusion of CO and production of both the 1,2-di-*tert*-butylcyclopentadienyl compound **B** and the skeletally rearranged 1,3-di-*tert*-butylcyclopentadienyl compound **C** in a 9:1

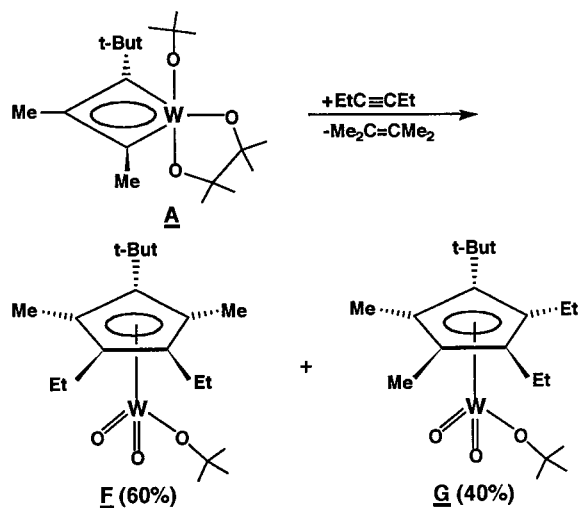
Scheme 25



Scheme 26



Scheme 27

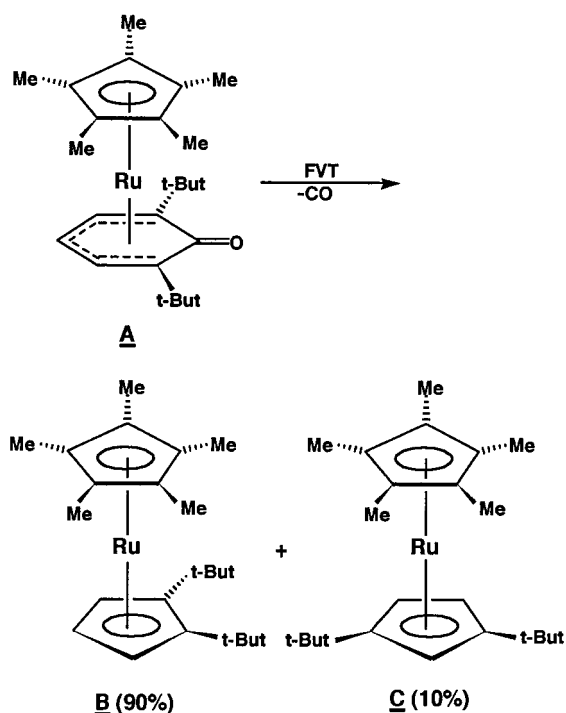


ratio. A possible pathway for this reaction (Scheme 29) involves the Dewar metallabenzene **D**, which can collapse to the major product **B** or isomerize to the metallacyclobutadiene-alkyne species **E**. Rotation of the alkyne and reformation of a Dewar metallabenzene (**G**) are followed by collapse to the minor product, **C**.

An alternative mechanism involving planar metallabenzenes that rearrange via a metallabenzvalene isomer (**I**) is also possible (Scheme 30). However, the formation of a planar metallabenzene from an η^5 -oxacyclohexadienyl ligand would require large changes in metal-carbon interactions; the proposed Dewar metallabenzene pathway (Scheme 29) is considerably less disruptive to the bonding.

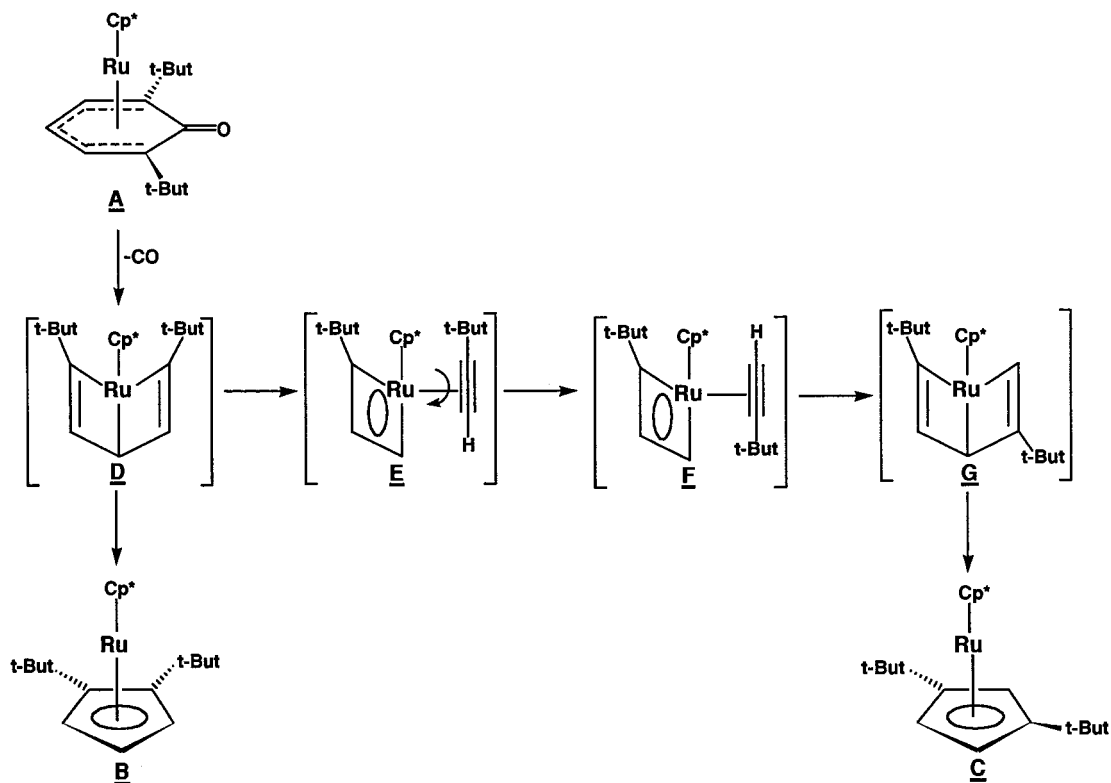
Interestingly, planar metallabenzenes have been rigorously *ruled out* as intermediates in several reactions that lead to cyclopentadiene-metal or

Scheme 28



cyclopentadienyl–metal products. For example, through a series of deuterium-labeling experiments, Hughes³⁸ showed that the conversion of the 1,3,4,5- η -pentadienediyl–Rh complex **A** (Scheme 31) to the η^4 -cyclopentadiene–Rh complex **B** cannot proceed through a *planar* metallacyclohexadiene or metallabenzene intermediate (**C** or **D**).³⁹ Rather, ring closure must involve direct C–C bond formation from the puckered ligand and is probably best regarded as an

Scheme 29



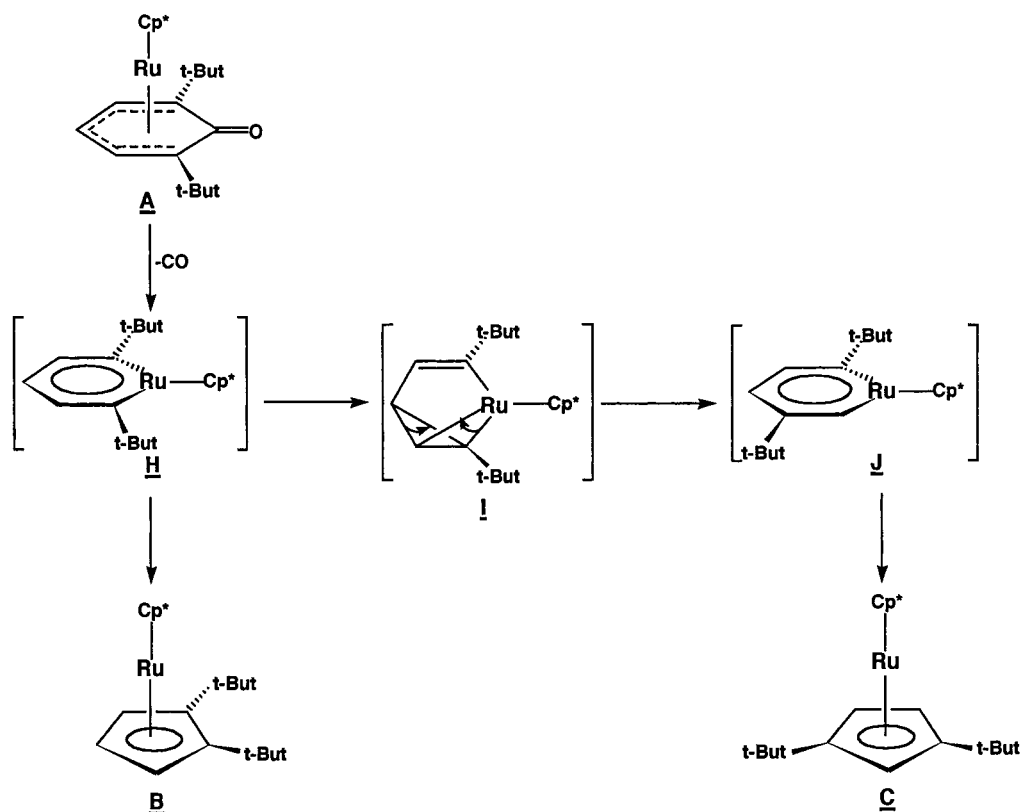
intraligand migratory insertion reaction. A similar result has been obtained for the conversion of (1,3,4,5- η -1,2,3-triphenylpentadienediyl)Ru(C₅Me₅)⁺ to (η^5 -1,2,3-triphenylcyclopentadienyl)Ru(C₅Me₅).⁴⁰ It is not clear whether these conclusions can be extended to related systems that are less sterically biased.

B. Metallabenzenes as Possible Intermediates in Other Reactions

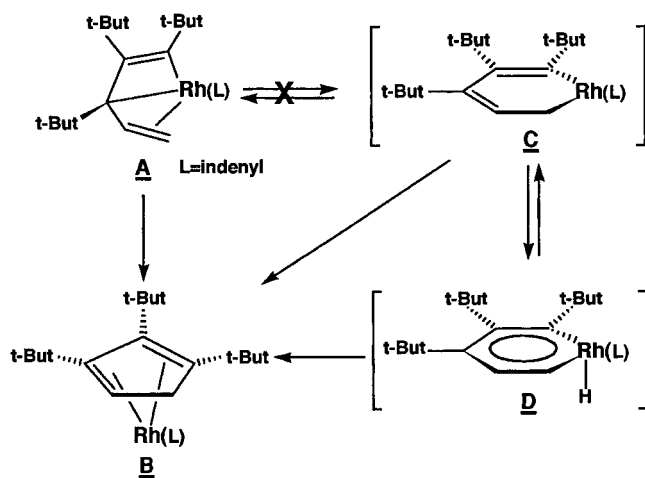
Metallabenzenes have been invoked as possible intermediates in several other reaction types. Schrock,⁴¹ for example, proposed tungstenabenzenes as possible intermediates in certain alkyne metathesis reactions that proceed by associative mechanisms. Shown in Scheme 32 is a proposed sequence for the metathesis of 3-heptyne to 3-hexyne and 4-octyne using a tungstenacyclobutadiene complex as catalyst. The postulated metallabenzenes are formed by alkyne insertion into the metal carbon bonds of the metallacyclobutadienes. Of course, it is also possible to envisage a catalytic cycle based on Dewar metallabenzene intermediates.

Similarly, Katz^{42,43} postulated that metallabenzenes might be intermediates in couplings of metal–carbynes with dialkynes, leading to the production of phenols. As shown in Scheme 33, the initial metal–carbyne/alkyne coupling would generate metallacyclobutadiene intermediate **A**. Insertion of the second alkyne moiety would produce transient metallabenzene **B**. Finally, carbonyl insertion and C–C coupling would lead to the ultimate phenol product. This final conversion (**B** → **C**) is reminiscent of the reaction of iridabenzene **5** with excess CO, which leads to a phenoxide product (cf. Scheme 7).

Scheme 30



Scheme 31



IX. Other Metal-Coordinated Metallabenzenes

As discussed earlier (section V), "iridabenzene" can be coordinated to a $\text{Mo}(\text{CO})_3$ moiety by arene exchange chemistry. However, a number of other metal-coordinated metallabenzenes have been synthesized directly, i.e., without prior generation of the *free* metallabenzene.

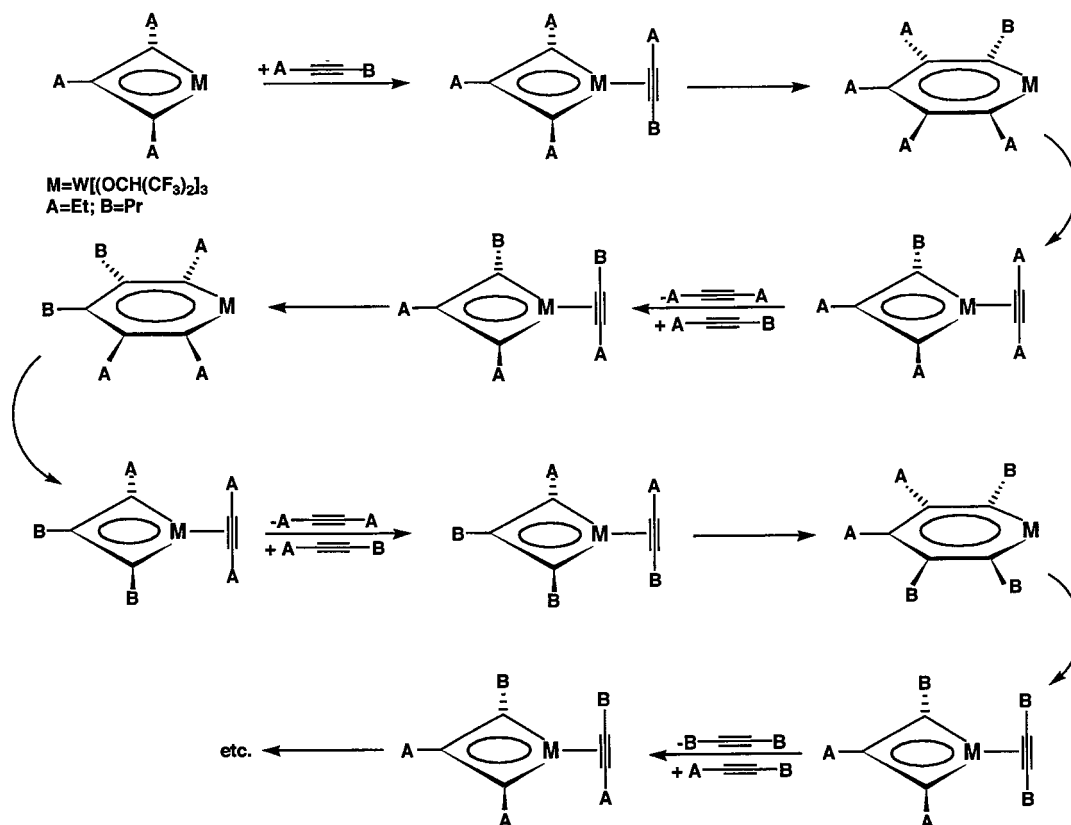
The first such example was reported in 1987 by Stone,⁴⁴ who isolated ferrabenzene complex **24** (Scheme 34) from the reaction of a bimetallic μ -carbyne complex **A** with 2 equiv of 2-butyne. This cyclization reaction is accompanied by hydrogen migrations between carbon atoms leading to the unexpected substitution pattern on the ferrabenzene ring. The ferrabenzene ligand serves as a neutral $6e^-$

donor, enabling the tungsten center to achieve an $18e^-$ count.

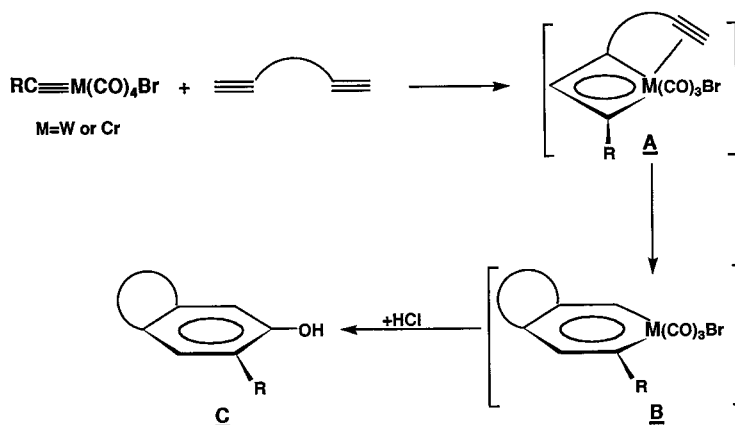
The C–C bond lengths within the ferrabenzene ring are equivalent within experimental error, indicating substantial π -electron delocalization (Table 3). Similarly, the Fe–C distances are essentially the same (2.072(5) and 2.051(5) Å) and short enough to suggest some multiple bond character. Perhaps the most striking structural feature is the pronounced displacement of the iron atom out of the ferrabenzene ring. The iron atom lies 0.80 Å out of the plane defined by C1/C2/C3/C4/C5 (and away from the W atom), resulting in a dihedral "fold" angle of 33.6° between this plane and the C1/Fe/C5 plane. This atom displacement probably results primarily from steric interactions, but there may be other subtle benefits. For example, metal atom displacement causes the internal angles at the α -carbons to be reduced and their p orbitals to point more directly toward the complexing metal center. It is interesting that the shortest W–C_{ring} bonds in **24** are with C1 and C5, while the longest bond is with C3 (Table 3). This contrasts with the situation in (iridabenzene)- $\text{Mo}(\text{CO})_3$, **11**, where Mo–C3 is the shortest Mo–C_{ring} bond. The shifting of the tungsten atom toward C1/C5 is probably a consequence of the fact that the iron atom is displaced significantly out of the ring; hence, tungsten must move toward it to form a strong M–M bond.

In the ^1H NMR spectrum of **24**, the lone ring proton, H3, appears at δ 4.69. In the ^{13}C NMR, the five ring carbons resonate between δ 90.2 and 130.7, with the α -carbons appearing farthest downfield, as expected (Table 4).

Scheme 32



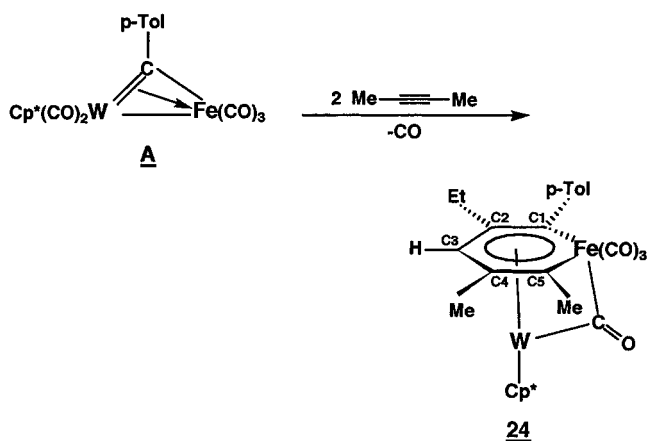
Scheme 33



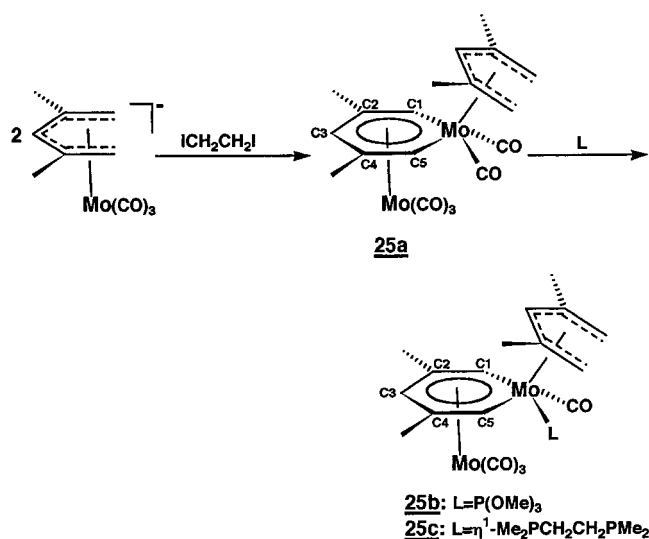
Ernst reported isolation of the metal-coordinated molybdenabenzene complex, **25a** (Scheme 35), from the reaction of 2 equiv of (η^5 -2,4-dimethylpentadienyl)- $Mo(CO)_3^-$ with 1,2-diiodoethane.^{45,46} Although the detailed mechanism of this reaction is not known, one of the pentadienyl ligands loses a hydrogen atom from each of its terminal carbon atoms to become the carbon portion of the metallabenzene ring. This type of hydrogen loss from pentadienyl ligands has previously been observed in the mass spectra of “half-open” and “open” metallocenes.^{45,47} As in the previous example, the metallabenzene serves as a $6e^-$ neutral ligand, enabling the second molybdenum atom to achieve an $18e^-$ count.

The bonding within the metallabenzene ring is delocalized (Table 3), and the $Mo-C_\alpha$ bond distances

Scheme 34



Scheme 35



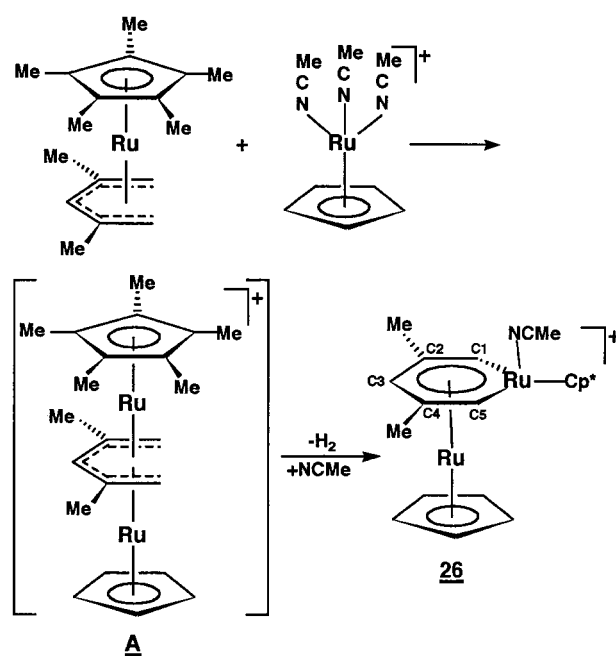
(2.150(5) and 2.161(4) Å) suggest some metal participation in ring π -bonding. The metallabenzene Mo center resides 0.33 Å out of the plane made by C1/C2/C3/C4/C5, resulting in a relatively modest dihedral “fold” angle of 11.6° between this plane and plane C1/Mo/C5. As expected, the ring protons on the molybdenabenzene ligand H1, H3, and H5, resonate downfield at δ 8.31, 5.74, and δ 6.91, respectively, in the ^1H NMR spectrum (Table 4).

Compound **25a** undergoes ligand substitution reactions when treated with trimethyl phosphite or bis(dimethylphosphino)ethane (Scheme 35). In each case, one of the CO ligands on the metallabenzene Mo atom is replaced with the phosphorus-based ligand, generating **25b** and **25c**. The position of this substitution can be readily rationalized; the metallabenzene Mo atom has a higher oxidation state (Mo(II)) than the other Mo atom (Mo(0)) and hence is a less effective back-bondor to CO. As a result, the carbonyls on the metallabenzene Mo are less tightly bound and more easily substituted. Although X-ray structures of the ligand-substituted derivatives, **25b,c**, have not been obtained, NMR data are fully consistent with retention of the aromatic ring (Table 4).

Salzer⁴⁸ produced metal-coordinated metallabenzene **26** (Scheme 36) by treating $(\eta^5\text{-}2,4\text{-dimethylpentadienyl})(\eta^5\text{-C}_5\text{Me}_5)\text{Ru}$ with the labile precursor $[(\eta^5\text{-C}_5\text{H}_5)\text{Ru}(\text{CH}_3\text{CN})_3]^+\text{PF}_6^-$. The triple-decker complex **A** may serve as an intermediate in this reaction. Loss of two hydrogen atoms from the terminal carbons of the central pentadienyl would lead to the coordinated ruthenabenzene product. The ruthenabenzene ligand serves as a $6e^-$ neutral donor, allowing the central ruthenium atom (which carries the compound's formal charge) to achieve an $18e^-$ count.

Structural and spectroscopic data for **26** are reported in Tables 3 and 4. As with earlier metal-coordinated metallabenzenes, the ring metal atom in **26** is significantly displaced out of the plane of the ring carbons and away from the second Ru atom resulting in a dihedral “fold” angle of 27.0° between planes C1/C2/C3/C4/C5 and C1/Ru/C5. This displacement is probably due primarily to strong steric

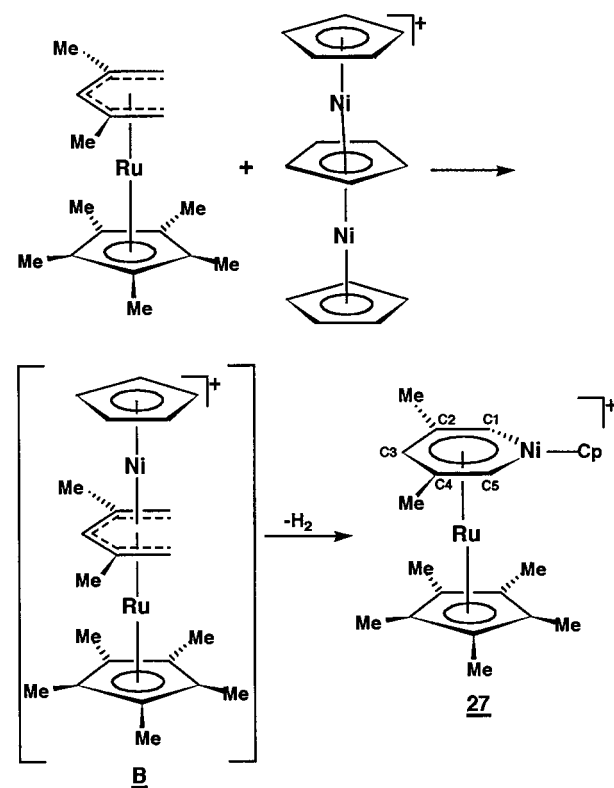
Scheme 36



interactions between the cyclopentadienyl and pentamethylcyclopentadienyl ligands (which lie in approximately perpendicular planes), but other subtle effects may also be in play (vide supra).

A ruthenium-coordinated nickelabenzene complex, **27** (Scheme 37), has also been synthesized by Salzer,

Scheme 37



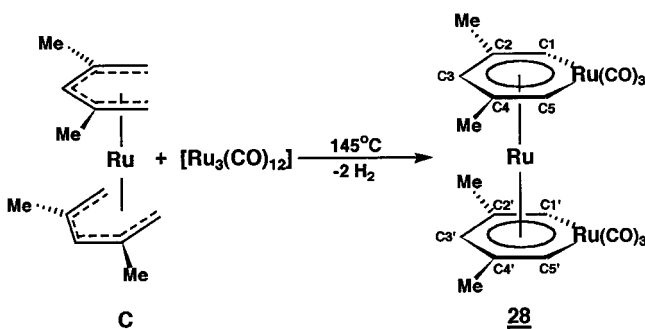
using a similar approach.⁴⁹ In this case, $(\eta^5\text{-}2\text{-}4\text{-dimethylpentadienyl})(\eta^5\text{-C}_5\text{Me}_5)\text{Ru}$ is treated with $[(\eta^5\text{-C}_5\text{H}_5)\text{Ni}(\eta^5\text{-C}_5\text{H}_5)\text{Ni}(\eta^5\text{-C}_5\text{H}_5)]^+$, which serves as a labile source of the $14e^-$ fragment $(\eta^5\text{-C}_5\text{H}_5)\text{Ni}^+$.

Again, a triple-decker species, **B**, in which a 2,4-dimethylpentadienyl group serves as the central ligand, may be involved as an intermediate. The metallabenzene ligand in **27** again serves as a $6e^-$ neutral donor, enabling the central ruthenium center (formally a cation) to achieve an $18e^-$ count.

Structural and spectroscopic data for compound **27** are reported in Tables 3 and 4. The metallabenzene ring is still somewhat nonplanar, but the displacement of the nickel atom out of the ring (and away from ruthenium) is less pronounced than is the displacement of Ru in **26**; the dihedral "fold" angle between C1/C2/C3/C4/C5 and C1/Ni/C5 is 16.4° vs 27.0° for the analogous angle in **26**. Salzer⁴⁹ suggested that this reduced displacement results from the fact that the optimal Ru–Ni distance is shorter than the optimal Ru–Ru distance. However, Girolami⁵⁰ pointed out that, in general, shorter M–M bonds do *not* correlate with smaller metal displacements and reduced folding angles in metal-coordinated metallabenzene rings. He concludes that the smaller displacement results from reduced steric interactions between the ligands on the two metal centers.

Recently, Salzer⁵¹ succeeded in generating the first example of a homoleptic metallabenzene sandwich compound, **28** (Scheme 38). This was accomplished

Scheme 38



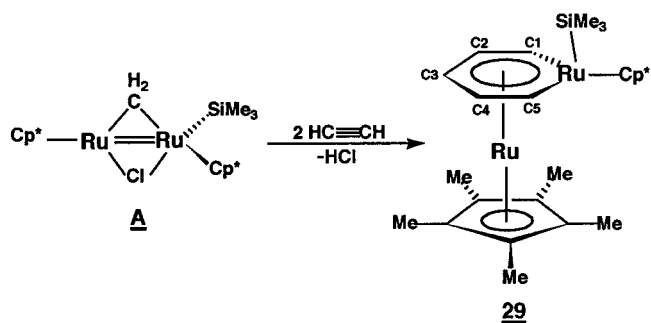
by treating the open ruthenocene **C** with $\text{Ru}_3(\text{CO})_{12}$ at 145°C . The electron counting in **28** is somewhat different than that in the previously discussed metal-coordinated metallabenzenes. If the metallabenzene ligands are counted as neutral $6e^-$ donors, the central ruthenium is then formally $20e^-$ (and the metallabenzene rutheniums are $17e^-$). Hence, a better approach in this case is to assign the metallabenzene ligands a negative charge and count them as anionic $6e^-$ donors, much like boratabenzene ($\text{C}_5\text{H}_5\text{BH}^-$). The central ruthenium ion is then $\text{Ru}(\text{II}) \equiv d^6$ and has an 18 valence electron count. The ruthenium atoms in the anionic metallabenzene ligands are formally $\text{Ru}(0) \equiv d^8$ and are likewise $18e^-$ centers. The negative charges on the metallabenzene ligands may explain the unusually upfield chemical shift observed for the α -H's of the ring in the ^1H NMR spectrum, $\delta 5.62$.

While the Ru–C $_{\alpha}$ distances within the metallabenzenes in **28** are somewhat longer than those in ruthenabenzene **26** (Table 3), they are still consistent with some multiple bond character. Carbon–carbon bonds are delocalized, as expected. The two metallabenzene rings are syn-eclipsed, and their ruthenium

ends tilt toward each other by 18° . The ruthenium atoms, however, are displaced slightly out of their metallabenzene rings and away from each other; the dihedral "fold" angles between planes C1/C2/C3/C4/C5 and C1/Ru/C5 are 15.1° and 12.9° for the two rings. The syn-eclipsed conformation allows for a possible weak interaction *between* the two metallabenzene ruthenium atoms (Ru–Ru = $3.382(2)$ Å). On the basis of the infrared spectrum, the syn-eclipsed geometry appears to persist in solution.

Girolami^{50,52} succeeded in synthesizing the first example of a metallabenzene complex with no substituents (only H's) on its carbon framework. This species, compound **29** in Scheme 39, was isolated

Scheme 39



from the reaction of a methylene-bridged diruthenium precursor, **A**, with 2 equiv of ethyne. Cyclization of the ruthenium–methylene moiety and the acetylenes, together with loss of HCl, leads to the production of **29**. When the reaction is carried out with ethyne- d_2 , the tetradeuterated metallabenzene product is obtained. One of the two hydrogen atoms of the bridging methylene group is retained, and it resides exclusively in an *ortho* position of the ruthenabenzene ring. This strongly suggests that the elimination of HCl takes place *after* the insertion of both acetylene molecules into the ruthenium–methylene unit and rules out the intermediacy of a symmetrical metallacyclobutadiene intermediate. As in **28**, the metallabenzene ligand in **29** is probably best regarded as an anion. In this view, the central ruthenium ion is then $\text{Ru}(\text{II}) \equiv d^6$ and has an $18e^-$ count, while the metallabenzene ruthenium center is likewise an $18e^-$ $\text{Ru}(\text{II}) \equiv d^6$ ion.

The structural features of **29** (Table 3) are fully consistent with the metallabenzene formulation. The ring ruthenium atom sits 0.32 Å out of the ring carbon plane, leading to a modest dihedral "fold" angle of 13° between planes C1/C2/C3/C4/C5 and C1/Ru/C5. The ring protons in **29** resonate downfield in the ^1H NMR spectrum, with H1, H2, and H3 appearing at $\delta 9.75$, 4.94 , and 4.32 , respectively.

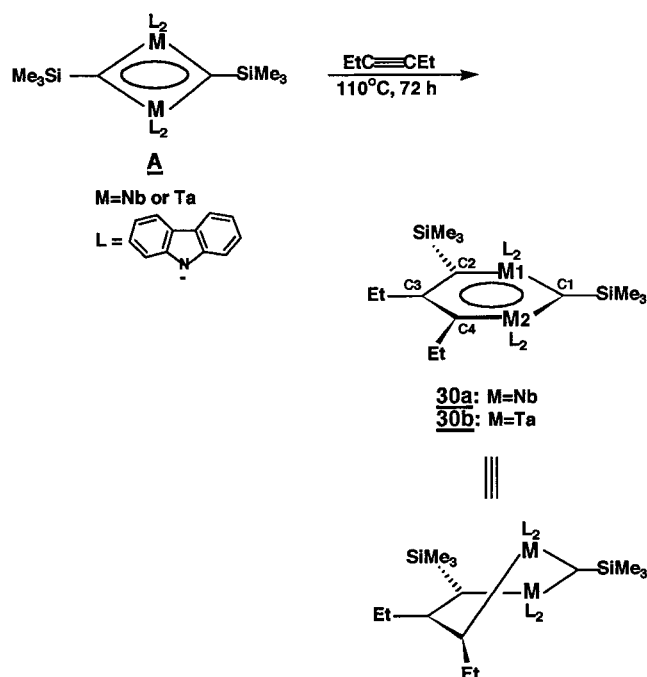
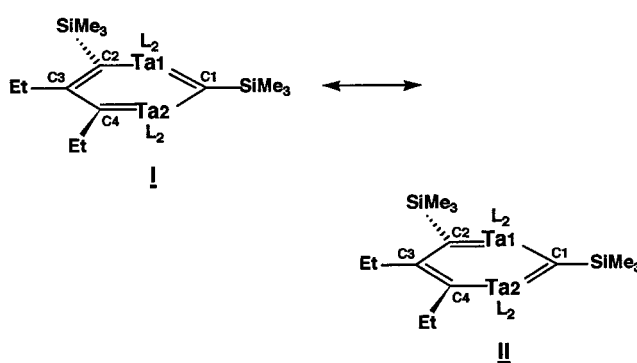
X. Dimetallabenzenes

A family of dimetallabenzenes has been synthesized by Rothwell et al.^{53,54} These species are generated by treating dimetallacyclobutadienes with alkynes at high temperatures. For example, treatment of the diniobiacyclobutadiene or ditantalacyclobutadiene complexes **A** (Scheme 40) with 3-hexyne generates dimetallabenzenes **30a,b**, respectively.⁵⁵

Table 5. Structural Data for Dimetallabenzenes^a

cmpd no.	bond distances (Å)					
	M1–C1	M1–C2	M2–C1	M2–C4	C2–C3	C3–C4
30b	1.99(2)	2.11(2)	2.04(2)	2.04(2)	1.40(3)	1.48(3)
31a	1.975(9)	2.03(1)	2.026(9)	2.04(1)	1.41(1)	1.40(1)
31b	1.988(8)	2.058(8)	1.998(7)	2.033(7)	1.41(1)	1.42(1)
32	1.989(6)	2.032(7)	2.005(6)	2.031(6)	1.43(1)	1.42(1)

cmpd no.	bond angles (deg)					
	C1–M1–C2	M1–C2–C3	C2–C3–C4	C3–C4–M2	C4–M2–C1	M2–C1–M1
30b	102.8(7)	93(1)	119(2)	98(1)	99.6(7)	90.5(7)
31a	99.3	95.8(6)	121.3(9)	93.0(6)	99.9	91.5(4)
31b	99.3	95.3(5)	124.9(7)	93.1(5)	101.7	92.5(3)
32	102.9(3)	100.6	126.9(6)	96.3(4)	103.1(3)	95.6(3)

^a See schemes for atom labeling.**Scheme 40****Chart 6. Resonance Structures for Compound 30b****Table 6. NMR Chemical Shift Data for Dimetallabenzenes (δ)^a**

cmpd no.	H3	C1	C2	C3	C4
30a		X	X	X	X
30b		393.0	253.9	X	257.3
31a	8.43	X	267.9	X	267.9
31b	8.64	386.5	255.0	X	255.0
32	9.03	361.1	239.2	X	239.2

^a See schemes for atom labeling. "X" indicates that the data were not reported.

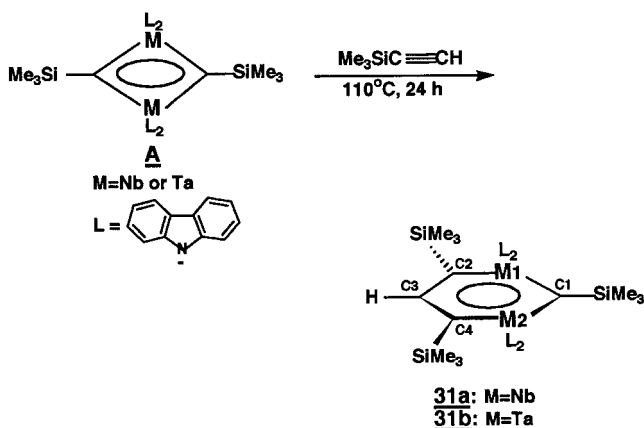
Mechanistically, these reactions probably proceed by alkyne insertion into a M–C bond; however, cycloaddition and formation of a Dewar dimetallabenzene intermediate cannot be ruled out.

The X-ray crystal structure of **30b** shows the six-membered metallacycle to be significantly distorted from planarity; the (Et)CC(Et)C(SiMe₃) unit is twisted by 53° with respect to the (L₂)TaC(SiMe₃)TaL₂ moiety. As reported in Table 5, the internal angles within the dimetallabenzene ring sum to 602.9°, a substantial deviation from the value of 720° required for a planar hexagon. From NMR studies, the energy required for metallacycle **30b** to achieve planarity before flipping into the other enantiomeric form is estimated to be 16.1(5) kcal/mol. The bond lengths around the ring (Table 5) reflect some delocalization, but resonance structure **I** (Chart 6) appears to be a stronger contributor than **II**.

NMR data for dimetallabenzenes are reported in Table 6. Ring carbon C1 in **30b** is shifted far downfield (δ 393.0), reflecting its close proximity to both metal centers. Carbons C2 and C4 resonate at

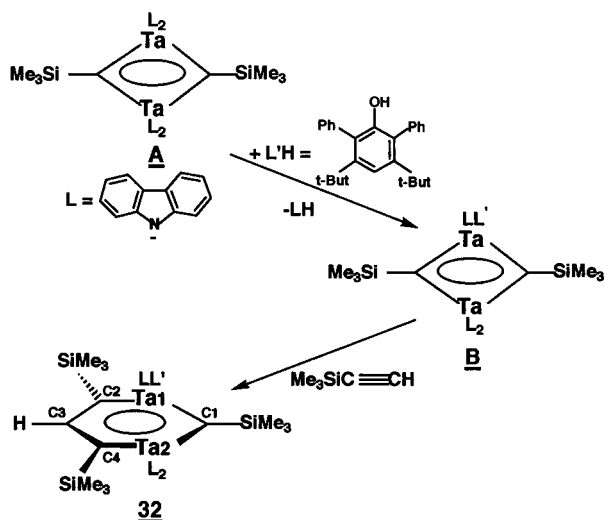
δ 253.9 and 257.3, while the chemical shift position of C3 is not reported.

Treatment of dimetallacyclobutadiene reagents **A** (Scheme 41) with the terminal alkyne, Me₃SiC≡CH,

Scheme 41

produces dimetallabenzenes **31a,b**. Only the sym-

Scheme 42



metrical regioisomer with the TMS groups on alternating ring atoms is produced, probably for steric reasons. In this isomer, the two resonance structures are equivalent, so the ring bonding is expected to be more delocalized than in **30b**. This is indeed the case for both **31a** and **31b**, which have been structurally characterized (see Table 5). Both molecules are significantly twisted; the dihedral angles between planes M1/C1/M2 and C2/C3/C4 are in the range of 52–57°. In the ^1H NMR (Table 6), the ring proton (H3) in **31a** and **31b** appears at δ 8.43 and 8.64, respectively, consistent with the presence of an aromatic ring current. However, the interpretation is complicated by the fact that this ring proton resides β to two metal centers and the observed downfield shift may be due primarily to metal-based anisotropy. Furthermore, because the rings are so severely distorted from planarity, the π -orbital overlap required for the establishment of a ring current is expected to be weak.

A closely related ditantalabenzene, **32** (Scheme 42), has been synthesized by first replacing one of the carbazole ligands in the precursor ditantalacyclobutadiene with a 3,5-di-*tert*-butyl-2,6-diphenylphenoxide ligand and then treating this species (**B**) with $\text{Me}_3\text{SiC}\equiv\text{CH}$. Compound **32** has structural and spectroscopic features that closely resemble those of **31a,b** (see Tables 5 and 6).

XI. Summary

Many similarities exist between metallabenzene and conventional arenes. Among these similarities are structural features such as ring planarity and the absence of bond length alternation, spectroscopic features such as downfield chemical shifts for ring protons, and chemical reactions such as electrophilic aromatic substitution and arene displacement from $(\text{arene})\text{Mo}(\text{CO})_3$. All of these features, taken together, strongly support the thesis that metallabenzene represents a new class of aromatic compounds, one in which metal d orbitals participate fully with carbon p orbitals in the formation of ring π -bonds.

However, it is also apparent that metallabenzene are much more prone to isomerization reactions than

are conventional arenes. This appears to be particularly true of first-row and second-row metallabenzene, where the metal–carbon bond strengths are weaker.⁵⁶ In these systems, carbene migratory insertion often leads to cyclopentadienyl–metal products.

π -Coordination of metallabenzene to other metal centers generally stabilizes the metallabenzene moieties while maintaining their aromatic character.⁵⁷ Among metallabenzene coordinated in this way, there are representatives from all three transition-metal rows (Fe, Ni, Mo, Ru, and Ir). The metal atom in π -coordinated metallabenzene is displaced out of the ring and away from the complexing metal center. The reason for this displacement in most cases appears to be steric repulsion between ligands on the two metal centers. However, other subtle effects may contribute. For example, metal displacement leads to more favorable internal angles at the α -carbons and a better orientation of C_α p orbitals toward the complexing metal center.

While no dominant synthetic strategy for constructing metallabenzene has emerged, cyclization reactions involving metal–thiocarbonyl, metal–alkylidyne, and metal–alkylidene precursors have proved useful. In addition, approaches involving pentadienyl reagents as the source of ring carbons have yielded notable successes. Vinylcyclopropene reagents have recently led to isolation of the first example of a metallabenzene valence isomer—a metallabenzvalene—and its subsequent conversion to a planar metallabenzene. Finally, interligand attacks of butadienyls on carbonyls have produced a variety of transient oxy- or alkoxy-substituted metallabenzene species. The development of new synthetic approaches, particularly systematic approaches that can be used with a variety of transition metals, is the key issue facing metallabenzene chemists.

One hundred and thirty-five years after Kekulé's celebrated dream, aromatic chemistry continues to be a fascinating and provocative research topic. Metallabenzene represents one of the "new frontiers" that promise to keep aromatic chemistry vibrant well into the 21st century.

XII. Acknowledgments

I would like to thank the many talented students who have contributed to the study of metallabenzene and related compounds in my laboratory. In addition, I am grateful to the principal sponsors of this research—the National Science Foundation and the Petroleum Research Fund, administered by the American Chemical Society. Finally, I wish to acknowledge Dr. Nigam Rath, Department of Chemistry, University of Missouri–St. Louis, for his help in obtaining some of the X-ray structural data that are included in this review.

XIII. References

- (1) Kekulé, A. *Bull. Soc. Chim.* **1865**, 3, 98–111.
- (2) (a) Badger, G. M. *Aromatic Character and Aromaticity*; Cambridge University Press: London, 1969. (b) *Aromaticity, Pseudo-Aromaticity, Anti-Aromaticity*; Bergmann, E. D., Pullman, B., Eds.; Academic Press: New York, 1971. (c) Garratt, P. J. *Aromaticity*; John Wiley and Sons: New York, 1986. (d) Lloyd,

- D. *The Chemistry of Conjugated Cyclic Compounds*; John Wiley and Sons: Chichester, 1989.
- (3) "High thermodynamic stability" simply means more stable than the canonical form of lowest energy. It does not imply stability to air, light, or common reagents. See: March, J. *Advanced Organic Chemistry*, 3rd ed.; John Wiley and Sons: New York, 1985; pp 37–39.
 - (4) (a) Ashe, A. J., III *Acc. Chem. Res.* **1978**, *11*, 153–157. (b) Jutzi, P. *Angew. Chem., Int. Ed. Engl.* **1975**, *14*, 232–245.
 - (5) Ashe, A. J., III *Angew. Chem., Int. Ed. Engl.* **1995**, *34*, 1357–1359.
 - (6) (a) Chen, J.; Daniels, L. M.; Angelici, R. J. *J. Am. Chem. Soc.* **1990**, *112*, 199–204. (b) Chin, R. M.; Jones, W. D. *Angew. Chem., Int. Ed. Engl.* **1992**, *31*, 357–358. (c) Bianchini, C.; Meli, A.; Peruzzini, M.; Vizza, F.; Frediani, P.; Herrera, V.; Sanchez-Delgado, R. A. *J. Am. Chem. Soc.* **1993**, *115*, 2731–2742. (d) Bianchini, C.; Meli, A.; Peruzzini, M.; Vizza, F.; Moneti, S.; Herrera, V.; Sanchez-Delgado, R. A. *J. Am. Chem. Soc.* **1994**, *116*, 4370–4381. (e) Bleeke, J. R.; Hinkle, P. V. *J. Am. Chem. Soc.* **1999**, *121*, 595–596. For a good theoretical discussion, see: Palmer, M.; Carter, K.; Harris, S. *Organometallics* **1997**, *16*, 2448–2459.
 - (7) (a) Bleeke, J. R.; Blanchard, J. M. B. *J. Am. Chem. Soc.* **1997**, *119*, 5443–5444. (b) Bleeke, J. R.; Blanchard, J. M. B.; Donnay, E. *Organometallics* **2001**, *20*, 324–336.
 - (8) Weller, K. J.; Filippov, I.; Briggs, P. M.; Wigley, D. E. *Organometallics* **1998**, *17*, 322–329. For an example of a metalla-pyrimidine, see: Feng, S. G.; White, P. S.; Templeton, J. L. *Organometallics* **1993**, *12*, 1765–1774.
 - (9) Thorn, D. L.; Hoffman, R. *Nouv. J. Chim.* **1979**, *3*, 39–45.
 - (10) Jorgensen, W. L.; Salem, L. *The Organic Chemist's Book of Orbitals*; Academic Press: New York, 1973, p 240.
 - (11) Schleyer, P. v. R.; Wang, Z.-X. Personal communication.
 - (12) A similar conclusion has been reached by using molecular hardness as a criterion for aromaticity. See: Chamizo, J. A.; Morgado, J.; Sosa, P. *Organometallics* **1993**, *12*, 5005–5007.
 - (13) Elliott, G. P.; Roper, W. R.; Waters, J. M. *J. Chem. Soc., Chem. Commun.* **1982**, 811–813.
 - (14) Elliott, G. P.; Mcauley, N. M.; Roper, W. R. *Inorg. Synth.* **1989**, *26*, 184–189.
 - (15) Rickard, C. E. F.; Roper, W. R.; Woodgate, S. D.; Wright, L. J. *Angew. Chem., Int. Ed. Engl.* **2000**, *39*, 750–752.
 - (16) Bleeke, J. R. *Acc. Chem. Res.* **1991**, *24*, 271–277.
 - (17) Bleeke, J. R.; Behm, R.; Xie, Y.-F.; Chiang, M. Y.; Robinson, K. D.; Beatty, A. M. *Organometallics* **1997**, *16*, 606–623.
 - (18) Bleeke, J. R.; Xie, Y.-F.; Peng, W.-J.; Chiang, M. *J. Am. Chem. Soc.* **1989**, *111*, 4118–4120.
 - (19) (1,3,4,5- η -2,3-diphenylpentadienediyl)Rh(PMe₃)₃⁺ is similarly unreactive toward deprotonation. See: Hughes, R. P.; Trujillo, H. A.; Egan, J. W., Jr.; Rheingold, A. L. *Organometallics* **1999**, *18*, 2766–2772.
 - (20) Hughes, R. P.; Trujillo, H. A.; Rheingold, A. L. *J. Am. Chem. Soc.* **1993**, *115*, 1583–1585.
 - (21) Hughes, R. P.; Trujillo, H. A.; Egan, J. W., Jr.; Rheingold, A. L. *J. Am. Chem. Soc.* **2000**, *122*, 2261–2271.
 - (22) Bleeke, J. R.; Xie, Y. F.; Bass, L.; Chiang, M. Y. *J. Am. Chem. Soc.* **1991**, *113*, 4703–4704.
 - (23) These same products are obtained under classical Friedel–Crafts conditions.
 - (24) Bleeke, J. R.; Behm, R.; Xie, Y.-F.; Clayton, T. W., Jr.; Robinson, K. D. *J. Am. Chem. Soc.* **1994**, *116*, 4093–4094.
 - (25) Bleeke, J. R.; Bass, L. A.; Xie, Y.-F.; Chiang, M. Y. *J. Am. Chem. Soc.* **1992**, *114*, 4213–4219.
 - (26) Alternatively, the carbonyl ligands may rotate via a turnstile mechanism. See: Cotton, F. A.; Wilkinson, G. *Advanced Inorganic Chemistry*, 4th ed.; Wiley: New York, 1980; pp 1218–1222.
 - (27) Bleeke, J. R.; Behm, R. *J. Am. Chem. Soc.* **1997**, *119*, 8503–8511.
 - (28) Gilbertson, R. D.; Weakley, T. J. R.; Haley, M. M. *J. Am. Chem. Soc.* **1999**, *121*, 2597–2598.
 - (29) Gilbertson, R. D.; Weakley, T. J. R.; Haley, M. M. *Chem. Eur. J.* **2000**, *6*, 437–441.
 - (30) Yang, J.; Jones, W. M.; Dixon, J. K.; Allison, N. T. *J. Am. Chem. Soc.* **1995**, *117*, 9776–9777.
 - (31) Ferede, R.; Allison, N. T. *Organometallics* **1983**, *2*, 463–465.
 - (32) Ferede, R.; Hinton, J. F.; Korfmacher, W. A.; Freeman, J. P.; Allison, N. T. *Organometallics* **1985**, *4*, 614–616.
 - (33) Mike, C. A.; Ferede, R.; Allison, N. T. *Organometallics* **1988**, *7*, 1457–1459.
 - (34) Yang, J.; Yin, J.; Abboud, K. A.; Jones, W. M. *Organometallics* **1994**, *13*, 971–978.
 - (35) Schrock, R. R.; Pederson, S. F.; Churchill, M. R.; Ziller, J. W. *Organometallics* **1984**, *3*, 1574–1583.
 - (36) Another possible explanation for the skeletal rearrangement is that metallacyclobutadiene **A** isomerizes to an η^3 -cyclopropenyl–metal complex upon addition of the alkyne and that the alkyne inserts into a M–cyclopropenyl σ -bond. The resulting β -cyclopropenylvinyl complex then rearranges to the observed cyclopentadienyl product.
 - (37) Hughes, R. P.; Kowalski, A. S. *Organometallics* **1998**, *17*, 270–273.
 - (38) Donovan, B. T.; Hughes, R. P.; Trujillo, H. A. *J. Am. Chem. Soc.* **1990**, *112*, 7076–7077.
 - (39) These kinds of intermediates had originally been suggested by Hughes and also by Bleeke in a related iridium system. See: (a) Egan, J. W., Jr.; Hughes, R. P.; Rheingold, A. L. *Organometallics* **1987**, *6*, 1578–1581. (b) Bleeke, J. R.; Peng, W.-J. *Organometallics* **1987**, *6*, 1576–1578.
 - (40) Hughes, R. P.; Trujillo, H. A.; Gauri, A. J. *Organometallics* **1995**, *14*, 4319–4324.
 - (41) Freudenberger, J. H.; Schrock, R. R.; Churchill, M. R.; Rheingold, A. L.; Ziller, J. W. *Organometallics* **1984**, *3*, 1563–1573.
 - (42) Sivavec, T. M.; Katz, T. J. *Tetrahedron Lett.* **1985**, *26*, 2159–2162.
 - (43) Sivavec, T. M.; Katz, T. J.; Chiang, M.; Yang, G. X.-Q. *Organometallics* **1989**, *8*, 1620–1625.
 - (44) Hein, J.; Jeffery, J. C.; Sherwood, P.; Stone, F. G. A. *J. Chem. Soc., Dalton Trans.* **1987**, 2211–2218.
 - (45) Kralick, M. S.; Rheingold, A. L.; Ernst, R. D. *Organometallics* **1987**, *6*, 2612–2614.
 - (46) Kralick, M. S.; Rheingold, A. L.; Hutchinson, J. P.; Freeman, J. W.; Ernst, R. D. *Organometallics* **1996**, *15*, 551–561.
 - (47) Thermal conversion of pentadienyl ligands to cyclopentadienyl ligands with hydrogen elimination is also known. (a) Mann, B. E.; Manning, P.; Spencer, C. M. *J. Organomet. Chem.* **1986**, *312*, C64–C66. (b) Kirss, R. U. *Organometallics* **1992**, *11*, 497–499. (c) Kirss, R. U.; Quazi, A.; Lake, C. H.; Churchill, M. R. *Organometallics* **1993**, *12*, 4145–4150.
 - (48) Bosch, H. W.; Hund, H.-U.; Nietlispach, D.; Salzer, A. *Organometallics* **1992**, *11*, 2087–2098.
 - (49) Bertling, U.; Englert, U.; Salzer, A. *Angew. Chem., Int. Ed. Engl.* **1994**, *33*, 1003–1004.
 - (50) Lin, W.; Wilson, S. R.; Girolami, G. S. *Organometallics* **1997**, *16*, 2356–2361.
 - (51) Englert, U.; Podewils, F.; Schiffrers, I.; Salzer, A. *Angew. Chem., Int. Ed. Engl.* **1998**, *37*, 2134–2136.
 - (52) Lin, W.; Wilson, S. R.; Girolami, G. S. *J. Chem. Soc., Chem. Commun.* **1993**, 284–285.
 - (53) Profflet, R. D.; Fanwick, P. E.; Rothwell, I. P. *Angew. Chem., Int. Ed. Engl.* **1992**, *31*, 1261–1263.
 - (54) Riley, P. N.; Profflet, R. D.; Salberg, M. M.; Fanwick, P. E.; Rothwell, I. P. *Polyhedron* **1998**, *17*, 773–779.
 - (55) Related reactions involving 1,3-ditungstenacyclobutadienes and alkynes have been studied. However, in these cases, a much more severe distortion is observed, leading to a structure best described as containing a dimetalated allyl ligand: Chisholm, M. H.; Huffman, J. C.; Heppert, J. A. *J. Am. Chem. Soc.* **1985**, *107*, 5116–5136. See also: Chisholm, M. H.; Jansen, R.-M.; Huffman, J. C. *Organometallics* **1992**, *11*, 2305–2307.
 - (56) Collman, J. P.; Hegedus, L. S.; Norton, J. R.; Finke, R. G. *Principles and Applications of Organotransition Metal Chemistry*; University Science Books: Mill Valley, CA, 1987; p 100.
 - (57) Some organic arenes appear to become more aromatic (based on "bond-fixing power") when π -complexed to a Cr(CO)₃ moiety. See: Mitchell, R. H.; Zhou, P.; Venugopalan, S.; Dingle, T. W. *J. Am. Chem. Soc.* **1990**, *112*, 7812–7813.

CR990337N

